WILEY-BLACKWELL

Cladistics (2020) 1–23

Cladistics

10.1111/cla.12431

Phylogeny of Lithobiidae Newport, 1844, with emphasis on the megadiverse genus *Lithobius* Leach, 1814 (Myriapoda, Chilopoda)

Anne-Sarah Ganske[a,b], Varpu Vahtera[c], László Dányi[d], Gregory D. Edgecombe[e] and Nesrine Akkari[a]*

[a]*Naturhistorisches Museum Wien, 3. Zoologische Abteilung, Burgring 7, 1010 Vienna, Austria;* [b]*Department of Integrative Zoology, University of Vienna, Althanstraße 14, Vienna, 1090, Austria;* [c]*Zoological Museum, Biodiversity Unit, University of Turku, Vesilinnantie 5, Turku, 20014, Finland;* [d]*Department of Zoology, Hungarian Natural History Museum, Baross u. 13, Budapest, 1088, Hungary;* [e]*Department of Earth Sciences, The Natural History Museum, Cromwell Road, London,, SW7 5BD, UK*

Accepted 29 June 2020

Abstract

Phylogenetic analyses based on molecular and morphological data were conducted to shed light on relationships within the mostly Palaearctic/Oriental centipede family Lithobiidae, with a particular focus on the Palaearctic genus *Lithobius* Leach, 1814 (Lithobiidae, Lithobiomorpha), which contains >500 species and subspecies. Previous studies based on morphological data resolved *Lithobius* as nonmonophyletic, but molecular-based phylogenetic analyses have until now sampled few species. To elucidate species inter-relationships of the genus, test the validity of its classification into subgenera, and infer its relationships with other Lithobiidae, we obtained molecular data (nuclear markers: 18S rRNA, 28S rRNA; mitochondrial markers: 16S rRNA, COI) and 61 morphological characters for 44 species of *Lithobius* representing four of its eight subgenera and nine other representatives of Lithobiidae. The data were analyzed phylogenetically using maximum-likelihood, parsimony and Bayesian inference. This study suggests that (i) a close relationship between *L. giganteus* and the pterygotergine *Disphaerobius loricatus* highlighted in recent morphological analyses is also strongly supported by molecular data, and Pterygoterginae is formally synonymized with Lithobiinae; (ii) the Oriental/Australian genus *Australobius* is consistently resolved as sister group to all other sampled Lithobiidae by the molecular and combined data; (iii) the subfamily Ethopolyinae may be paraphyletic; (iv) the genus *Lithobius* is nonmonophyletic; (v) the subgenera *Lithobius*, *Sigibius* and *Monotarsobius* are nonmonophyletic and should not be used in future taxonomic studies; and (vi) there are instances of cryptic species and cases in which subspecies should be elevated to full species status, as identified for some European taxa within *Lithobius*.

Introduction

The monophyletic centipede order Lithobiomorpha contains approximately 1100 valid species in nearly 130 genera and subgenera, classified in the two monophyletic families Lithobiidae Newport, 1844 and Henicopidae Pocock, 1901 (Edgecombe and Giribet, 2003, 2004, 2019; Zapparoli and Edgecombe, 2011). Whereas the Lithobiidae is distributed mainly in the Northern Hemisphere and a few mostly introduced species occur in South America, southern Africa and Australasia, the Henicopidae have a predominantly temperate Southern Hemisphere native distribution (Zapparoli and Edgecombe, 2011).

With approximately 1000 species and subspecies, the family Lithobiidae comprises approximately 91% of the known diversity of the Lithobiomorpha (Zapparoli and Edgecombe, 2011; Bonato et al., 2016). It is a challenging group at all systematic levels. Few phylogenetic studies have been undertaken on Lithobiidae, such that its subfamilies and many of its genera are of uncertain status with regards to their monophyly, and many of its species are in need of revision

*Corresponding author:
E-mail address: nesrine.akkari@nhm-wien.ac.at

(Edgecombe, 2007; Zapparoli and Edgecombe, 2011). By contrast, the systematics of its sister taxon Henicopidae is quite well understood, being a less diverse group and having been the subject of molecular phylogenetic studies (e.g. Edgecombe et al., 2002; Edgecombe and Giribet, 2003). The Lithobiidae is currently classified in six subfamilies, namely Lithobiinae Newport, 1844; Ethopolyinae Chamberlin, 1915; Gosibiinae Chamberlin, 1912; Pseudolithobiinae Matic, 1973; Pterygoterginae Verhoeff, 1933 and Watobiinae Chamberlin, 1912 (Zapparoli and Edgecombe, 2011). The classification of these subfamilies is based on few morphological characters, with no phylogenetic testing using DNA sequences except for just a few species of Lithobiinae and Ethopolyinae (e.g. Murienne et al., 2010).

The monophyly of Lithobiidae was supported by Koch and Edgecombe (2008) who conducted a cladistic analysis of Lithobiomorpha based on 40 morphological characters. These authors (Koch and Edgecombe, 2008) further recovered paraphyly of Lithobiinae, which is the most species-rich subfamily within the Lithobiidae, including approximately 900 species and subspecies in *c*. 100 genera and subgenera with a largely Holarctic distribution (Zapparoli and Edgecombe, 2011).

With approximately 500 species and subspecies, *Lithobius* Leach, 1814 is the most species-rich genus in the entire Chilopoda and the most challenging taxon of the Lithobiinae (Zapparoli and Edgecombe, 2011; Bonato et al., 2016). This genus is mostly Palaearctic, with some native species also distributed in North America (Zapparoli and Edgecombe, 2011). Classification of *Lithobius* into eight subgenera (namely *Lithobius* Leach, 1814; *Monotarsobius* Verhoeff, 1905; *Sigibius* Chamberlin, 1913; *Ezembius* Chamberlin, 1919; *Dacolithobius* Matic, 1961; *Tracolithobius* Matic, 1962; *Chinobius* Verhoeff, 1934; *Porobius* Attems, 1926 (Zapparoli and Edgecombe, 2011)) has relied mostly on diagnostic combinations of the same small set of characters. Foremost, among these characters are the number of antennal articles (*c*. 20 vs. 25 or more), number of ocelli, number of teeth on the forcipular dental margin (anterior margin of forcipular coxosternite), form of the porodonts (a large seta usually on each side of the forcipular teeth), presence or absence of projections on specific tergites, distinctness of an articulation on legs 1–12 and the number of spurs on the female gonopod (morphological terminology following Bonato et al., 2010). Although these combinations of characters are taxonomically practical, their polarity has not been tested, such that some plesiomorphies are used in diagnoses. Nevertheless, some of the subgenera display a measure of geographical coherence: for example, *Lithobius* s.s. and *Ezembius* are distributed to the west and east of the Urals, respectively (Eason, 1992).

In a morphological cladistic analysis, representative species of the lithobiid genera *Australobius* Chamberlin, 1920, *Hessebius* Verhoeff, 1941, *Harpolithobius* Verhoeff, 1904 and *Pleurolithobius* Verhoeff, 1899, were each allied to particular species within *Lithobius* (Koch and Edgecombe, 2008). A subsequent phylogenetic analysis with new detailed information from the peristomatic structures, namely the epipharynx and hypopharynx, mandibles and first maxillae from a sample including 33 representatives from four of the eight subgenera (*Lithobius*, *Monotarsobius*, *Sigibius*, *Ezembius*), further supported the polyphyly of the genus *Lithobius* (Ganske et al., 2018a,b). However, a phylogenetic study including six species of *Lithobius* together with three species of Ethopolyinae and one species of *Australobius* provided weak molecular support for monophyly of *Lithobius* (Murienne et al., 2010). The analyses conducted by Ganske et al. (2018a) also resolved the sampled subgenera of *Lithobius* as nonmonophyletic, except for the subgenus *Sigibius* under parsimony. However, morphology alone was not sufficient to resolve certain species inter-relationships except for a few species groups (see Ganske et al., 2018a). The study also included additional representatives from other lithobiid subfamilies and genera, and the data further support Ethopolyinae and Pterygoterginae to cluster within Lithobiinae (Ganske et al., 2018a).

In this study, we acquired molecular information from the nuclear 18S rRNA and 28S rRNA and the mitochondrial 16S rRNA and COI gene regions from 40 European, four North American and one Asian lithobiids, representing four of the six subfamilies of Lithobiidae. The remaining two subfamilies, Pseudolithobiinae and Watobiinae, include altogether approximately 12 mostly poorly known American and one SW Asian species from which fresh material, suitable for DNA extraction, could not be collected. We provide the first molecular data for the lithobiid subfamilies Gosibiinae and Pterygoterginae. The species sampling was focused on Europe because the Palaearctic has the greatest species diversity of Lithobiinae and species-level taxonomy is most refined among European species, including half of the known species of *Lithobius* (Zapparoli, 2003). The obtained dataset was supplemented with already available sequences of other species of the family Lithobiidae (in total 53 species, including 44 species of *Lithobius* that represent four of its eight subgenera), its sister group Henicopidae (e.g. Edgecombe and Giribet, 2004), and *Scutigera coleoptrata* (Linnaeus, 1758) (Scutigeromorpha) as outgroup. An existing morphological dataset based on 62 characters (Ganske et al., 2018a) was additionally included in the analyses and supplemented with new morphological data from additional species.

The molecular and morphological datasets were analyzed using maximum-likelihood (ML), parsimony and Bayesian inference (BI). The molecular datasets were aligned using different algorithms to compare the resulting trees and to search for repeated and/or conflicting topologies.

Three main objectives are targeted here: (i) reveal some of the phylogenetic relationships of the Lithobiidae, focusing mainly on Lithobiinae and in more detail *Lithobius*; (ii) understand the inter-relationships of mainly European species assigned to the genus *Lithobius*, because it is the most species-rich genus within the Lithobiidae; (iii) review the systematic status of the genus *Lithobius* and its subgenera *Lithobius*, *Monotarsobius* and *Sigibius*. The obtained data also have allowed the revision of the taxonomy of a few taxa, notably for the subspecies *L. tenebrosus setiger* and *L. variegatus rubriceps* and to unveil cryptic taxa within the species *L. crassipes* and *L. crassipesoides*.

Material & methods

Taxon sampling

The studied material (Table 1) includes 53 taxa of Lithobiidae belonging to the subfamilies Lithobiinae (47 spp.), Gosibiinae (one sp.), Ethopolyinae (four spp.) and Pterygoterginae (one sp.). Within Lithobiinae, the genera *Australobius*, *Harpolithobius* and *Sozibius* are included with one species each, whereas 44 species of *Lithobius* represent the subgenera *Lithobius* (34 spp.), *Monotarsobius* (six spp.), *Sigibius* (three spp.) and *Ezembius* (one sp.). All type species of the subfamilies (except Gosibiinae) and all those of the genera and subgenera are included, except for *Anopsobius*, *Sigibius*, *Disphaerobius* and *Ezembius*, for which we alternatively included well-studied representative species.

The sampling of fresh material suitable for DNA analyses of further lithobiine genera was geographically restricted (e.g. genera erected by Chamberlin with a main distribution in North or Central America; *Anodonthobius* Matic, 1983 from Anatolia; *Dakrobius* Zalesskaja, 1975 from far east Russia). Five species of the Henicopidae from both subfamilies, Anopsobiinae (2 spp.) and Henicopinae (3 spp.), are included. The outgroup is the scutigeromorph *Scutigera coleoptrata*. Voucher specimens are deposited at the Natural History Museum Vienna (NHMW), the Hungarian Natural History Museum Budapest (HNHM), the Zoological Museum of the University of Turku (ZMUT) and the Senckenberg Museum of Natural History Görlitz (SMNG) (Supplements 1, 2 and Ganske et al., 2018a,b).

Molecular data

All sequences are newly generated (Table 1: *) following the protocol below except for 36 sequences retrieved from GenBank. Vouchers of the studied molecular specimens are listed in Supplement 1.

Specimens were collected in 96% ethanol and kept at room temperature, 6 °C or −20 °C until needed. DNA was extracted from one to five legs using the NucleoSpin™ Tissue Kit (Macherey-Nagel, Düren, Germany), following the standard protocol for animal tissue. PCR amplification of the target genes was done with purified genomic DNA. 18S rRNA (~1800 bp) was amplified in three overlapping fragments using the primer pairs 1F/5R, 3F/18Sbi and 18Sa2.0/9R (Giribet et al., 1996; Whiting et al., 1997). The 28S rRNA fragment (330 bp) was amplified with primer pair 28Sa/28Sb (Whiting et al., 1997). The 16S rRNA fragment (~500 bp) with primer pair 16Sa/16Sb (Xiong and Kocher, 1991; Edgecombe et al., 2002) and COI (~670 bp) with primer pair LCO1490/HCOout (Folmer et al., 1994; Carpenter and Wheeler, 1999). The PCR reaction (total 23 µL) consisted of 2 µL template DNA, 7.5 µL MQ water, 12.5 µL MyTaq™ Red Mix (Bioline, London, UK) and 0.5 µL of each primer (10 µM). The PCR amplification cycle consisted of an initial denaturation of 1 min at 95 °C, followed by 35 or 40 (some COI sequences only) cycles of denaturation of 15 s at 95 °C, annealing of 15 s at 42–52 °C and extension of 10 s at 72 °C. The annealing temperatures for the primers were as follow: 18S rRNA between 49 and 52 °C, 28S rRNA at 49 °C, 16S rRNA between 42 and 43 °C, and COI between 44 and 45 °C. Visualization of PCR products was obtained with a 1–1.5% agarose gel electrophoresis illuminated by LED or UV light. The gel was stained with Midori Green Advanced DNA Stain (NIPPON Genetics Europe GmbH, Düren, Germany) or SYBR™ Gold Nucleic Acid Gel Stain (Invitrogen™, Molecular Probes™, Thermo Fisher Scientific Inc., Waltham, MA, USA). Purification of PCR products was done with the A'SAP PCR cleanup kit (ArcticZymes, Tromsø, Norway) following the manufacturer's protocol. Sanger sequencing was performed by Macrogen Inc. (The Netherlands). Chromatograms were visualized and assembled using SEQUENCHER 5.4.6 and GENEIOUS v.R6, R11 and Prime. New sequences are deposited in GenBank and their accession numbers are provided in Table 1.

Morphological data

We used the same set of characters and coding information for the sampled taxa as described in Ganske et al. (2018a; morphological character matrix available as Supplementary Material 2 therein) except

Table 1
Taxon sampling used in the analyses with GenBank accession codes for the molecular partitions. Vouchers are listed in Supplement 1 and 2.

	18S rRNA	*28S rRNA*	*16S rRNA*	*COI*
Lithobiomorpha				
Henicopidae Pocock, 1901				
Anopsobiinae Verhoeff, 1907				
Anopsobius neozelanicus Silvestri, 1909	AF173248.1	AF173274.1	AF334337.1	AF334313.1
Dichelobius flavens Attems, 1911	AY213720.1	AY213739.1	AY214367.1	AY214421.1
Henicopinae Pocock, 1901				
Henicops dentatus Pocock, 1901	AY213725.1	AY213742.1	AY214370.1	–
Lamyctes africanus (Porat, 1871)	AF173244.1	AF173276.1	AF334338.1	DQ201429.1
Paralamyctes validus Archey, 1917	AF173243.1	AF173278.1	AF334357.1	AF334329.1
Lithobiidae Newport, 1844				
Gosibiinae Chamberlin, 1912				
Arenobius manegitus (Chamberlin, 1911)	MT722015*	MT734867*	MT711284*	MT804331*
Ethopolyinae Chamberlin, 1915				
Bothropolys multidentatus (Newport, 1845)	MT722014*	MT734866*	MT711283*	MT804330*
Ethopolys xanti (Wood, 1862)	HM453235.1	–	HM453217.1	HM453308.1
Eupolybothrus fasciatus (Newport, 1845)	AY213718.1	AY213737.1	AY214365.1	AY214420.1
Eupolybothrus grossipes (C.L. Koch, 1847)	MT721980*	MT734832*	MT711249*	MT804306*
Lithobiinae Newport, 1844				
Australobius scabrior Chamberlin, 1920	AF173241.1	AF173272.1	DQ201424.1	DQ201428.1
Harpolithobius anodus (Latzel, 1880)	–	–	–	KX458732.1
Sozibius tuobukus (Chamberlin, 1911)	MT722011*	MT734863*	MT711280*	MT804328*
Lithobius Leach, 1804				
Subgenus *Lithobius* Leach, 1814				
Lithobius agilis C.L. Koch, 1847	MT721981*	MT734833*	MT711250*	MT804307*
Lithobius atkinsoni Bollmann, 1887	MT721982*	MT734834*	MT711251*	–
Lithobius borealis Meinert, 1868	MT721986*	MT734838*	MT711255*	MT804309*
Lithobius castaneus Newport, 1844	MT721975*	MT734827*	MT711244*	–
Lithobius cyrtopus Latzel, 1880	MT721996*	MT734848*	MT711265*	–
Lithobius dentatus C.L. Koch, 1844	MT722000*	MT734852*	MT711269*	MT804320*
Lithobius erythrocephalus C.L. Koch, 1847	MT721992*	MT734844*	MT711261*	MT804315*
Lithobius forficatus (Linnaeus, 1758)	MT722010*	MT734862*	MT711279*	MT804327*
Lithobius glacialis Verhoeff, 1937	MT722002*	MT734854*	MT711271*	MT804322*
Lithobius lapidicola Meinert, 1872	MT721989*	MT734841*	MT711258*	MT804312*
Lithobius latro Meinert, 1872	MT722003*	MT734855*	MT711272*	–
Lithobius lucifugus L. Koch, 1862	MT722016*	MT734868*	–	MT804332*
Lithobius lusitanus Verhoeff, 1925	MT721987*	MT734839*	MT711256*	MT804310*
Lithobius macilentus L. Koch, 1862	MT722008*	MT734860*	MT711277*	MT804326*
Lithobius melanops Newport, 1845	MT721988*	MT734840*	MT711257*	MT804311*
Lithobius mutabilis L. Koch, 1862	MT722004*	MT734856*	MT711273*	MT804323*
Lithobius muticus C.L. Koch, 1847	MT722005*	MT734857*	MT711274*	MT804324*
Lithobius nodulipes Latzel, 1880	MT722006*	MT734858*	MT711275*	–
Lithobius obscurus Meinert, 1872	AF334271.1	AF334292.1	AF334333.1	–
Lithobius pelidnus Haase, 1880	MT721997*	MT734849*	MT711266*	–
Lithobius peregrinus Latzel, 1880	MT721983*	MT734835*	MT711252*	MT804308*
Lithobius piceus Haase, 1880	MT721990*	MT734842*	MT711259*	MT804313*
Lithobius pilicornis Newport, 1844	MT721976*	MT734828*	MT711245*	MT804303*
Lithobius pygmaeus Latzel, 1880	MT722007*	MT734859*	MT711276*	MT804325*
Lithobius rubriceps Newport, 1845 stat. nov.	–	HM453241.1	AY084071.1	AF334311.1
Lithobius schuleri Verhoeff, 1925	MT721985*	MT734837*	MT711254*	–
Lithobius setiger Kaczmareck, 1977 stat. nov.	MT721999*	MT734851*	MT711268*	MT804319*
Lithobius silvivagus Verhoeff, 1925	MT722009*	MT734861*	MT711278*	–
Lithobius stygius Latzel, 1880	–	MT734869*	–	–
Lithobius tenebrosus Meinert, 1872	MT721998*	MT734850*	MT711267*	MT804318*
Lithobius tricuspis Meinert, 1872	MT721991*	MT734843*	MT711260*	MT804314*
Lithobius validus Meinert, 1872	MT722001*	MT734853*	MT711270*	MT804321*
Lithobius variegatus Leach, 1814	AF000773.1	AF000780.1	–	KX458661.1
Lithobius viriatus Sseliwanoff, 1880	MT721984*	MT734836*	MT711253*	–
Subgenus *Monotarsobius* Verhoeff, 1905				
Lithobius aeruginosus L. Koch, 1862	MT721974*	MT734826*	MT711243*	MT804302*
Lithobius austriacus (Verhoeff, 1937)	MT721977*	MT734829*	MT711246*	–
Lithobius crassipes L. Koch, 1862	MT721994*	MT734846*	MT711263*	MT804317*

Table 1
(Continued)

	18S rRNA	28S rRNA	16S rRNA	COI
Lithobius crassipesoides Voigtländer, Iorio, Decker & Spelda, 2017	MT721995*	MT734847*	MT711264*	–
Lithobius curtipes C.L. Koch, 1847	MT721979*	MT734831*	MT711248*	MT804305*
Lithobius holstii (Pocock, 1895)	HM453234.1	–	HM453216.1	HM453307.1
Subgenus *Sigibius* Chamberlin, 1913				
Lithobius burzenlandicus Verhoeff, 1931	MT722012*	MT734864*	MT711281*	–
Lithobius carinthiacus Koren, 1992	MT722013*	MT734865*	MT711282*	MT804329*
Lithobius microps Meinert, 1868	MT721993*	MT734845*	MT711262*	MT804316*
Subgenus *Ezembius* Chamberlin, 1919				
Lithobius giganteus Sseliwanoff, 1881	–	HM453244.1	HM453215.1	HM453306.1
Pterygoterginae Verhoeff, 1933				
Disphaerobius loricatus (Sseliwanoff, 1881)	MT721978*	MT734830*	MT711247*	MT804304*
Scutigeromorpha				
Scutigeridae Leach, 1814				
Scutigerinae Leach, 1814				
Scutigera coleoptrata (Linnaeus, 1758)	AF000772.1	AF000779.1	DQ222156.1	DQ201426.1

*New data from the present study.

for character 52, which codes for *Lithobius franciscorum* Dányi & Tuf, 2012 alone, thus uninformative and not used in this study. In total, we used 61 morphological characters. The taxonomic sampling was enriched with the taxa *Lamyctes africanus*, *Dichelobius flavens*, *Arenobius manegitus*, *Ethopolys xanti*, *Sozibius tuobukus*, *Lithobius atkinsoni*, *Lithobius borealis*, *Lithobius glacialis*, *Lithobius lusitanus*, *Lithobius melanops*, *Lithobius obscurus*, *Lithobius pilicornis*, *Lithobius pygmaeus*, *Lithobius schuleri*, *Lithobius silvivagus*, *Lithobius stygius*, *Lithobius setiger*, *Lithobius variegatus*, *Lithobius rubriceps*, *Lithobius viriatus*, *Lithobius crassipesoides* and *Lithobius carinthiacus*. In those cases, coding for external characters (chars. 1–16 and 36–61) was done using literature resources or based on new observations with light microscopy (see Supplement 3 for detailed coding information). Information on the morphology of the peristomatic structures (chars. 17–28), mandibles (chars. 26–28) and first maxillae (chars. 33–35) was obtained using scanning electron microscopy (SEM) as described in Ganske et al. (2018a,b). The SEM information for *L. obscurus* and *L. variegatus* was taken partly from Edgecombe et al. (2002) and Edgecombe and Giribet (2004). Vouchers for the additional specimens used for SEM in this study are listed in Supplement 2. Some species studied by Ganske et al. (2018a) were not included as we could not obtain material suitable for molecular analyses. These are as follows: *Eupolybothrus tridentinus* (Fanzago, 1874); *Hessebius plumatus* Zalesskaja, 1978; *Lithobius calcaratus* C.L. Koch, 1844; *Lithobius carinatus* L. Koch, 1862; *Lithobius fagei* Demange, 1961; *Lithobius franciscorum*; *Lithobius trebinjanus* Verhoeff, 1900; *Lithobius electus* Silvestri, 1935; *Neolithobius aztecus* (Humbert & Saussure, 1869); *Pleurolithobius patriarchalis* (Berlese, 1894); and *Pseudolithobius megaloporus* (Stuxberg, 1875).

Some character descriptions taken from Ganske et al. (2018a) are slightly edited to include novel states, especially for characters 37, 40, 53, 54 to accommodate additional species:

Character 37. Projections of posterolateral corners of tergites: (0) all rounded; (1) T9 rounded, T11, T13 with projections; (2) T9, T11, T13 with projections; (3) T6, T7, T9, T11, T13 with projection; **(4) T7, T9, T11, T13 with projections**.

Tergites 7, 9, 11 and 13 show projections in *L. silvivagus* (Verhoeff, 1925, p. 156; Matic, 1966, p. 132, fig. 50A), *L. variegatus* (Eason, 1964, pp 181–182, fig. 294; Iorio and Voigtländer, 2019, fig. 69) and *Henicops dentatus* (Hollington and Edgecombe, 2004, p. 5, fig. 3). This differs from the states described for character 37 in Ganske et al. (2018a) so state (4) is added.

Character 40. Tarsus of legs 1–12: (0) divided into two **or more** tarsal articles; (1) undivided.

Hollington and Edgecombe, (2004, p. 4) diagnose three tarsal articles for the *Henicops dentatus*-group. State (0) was adjusted to accommodate *H. dentatus*.

Character 53. Male 15th femora or prefemora with distal knob **or projection**: (0) absent; (1) present. Males of *S. tuobukus* show prominent longitudinal dorso-medial sulci and medio-distal projections on the 15th femora (Fig. 1A,B). These modifications were already described and illustrated by Chamberlin (1922, p. 264, plate 1, fig. 6), but our observations show that the distal projections are more complex. Character 37 is adjusted to accommodate this species.

Character 54. Male 14th/15th tibiae/femora with a circular protuberance **or depression** covered with setae: (0) absent; (1) present.

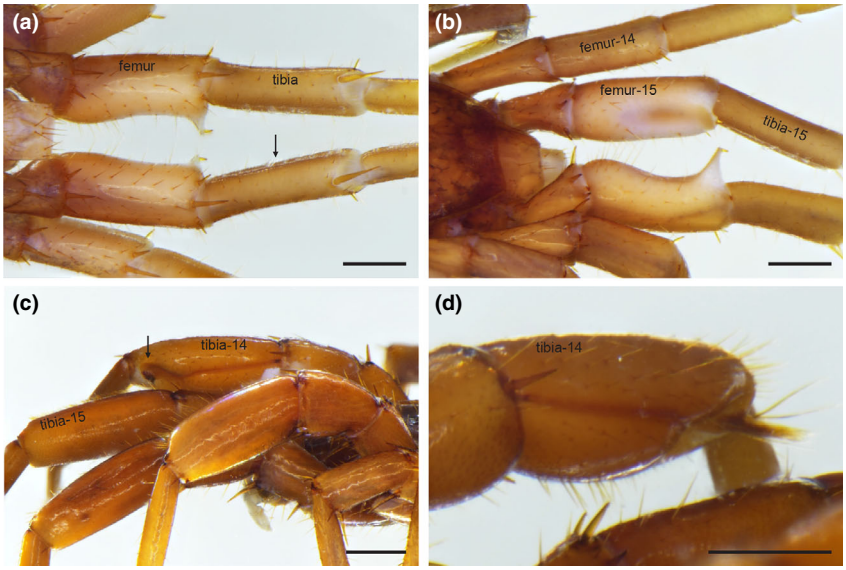

Fig. 1. Light microscopy photographs of modifications on 14th and 15th legs of male *Sozibius tuobukus* (a, b) and *Arenobius manegitus* (c, d). (a) 15th legs, ventral view, right is posterior, 15th femora with distal projection, arrow indicating median sulcus on the 15th tibia. (b) 14th and 15th legs, dorsolateral view, right is posterior, 15th femora with deep furrow and distal projections. (c) 14th and 15th legs, lateral view, left is posterior, 14th tibia with distal depression and tuft of setae (arrow). (d) 14th right tibia with longitudinal furrow and distal depression bearing a tuft of setae, lateral view, right is posterior. Scale bars = 500 μm.

The 14th tibiae of *A. manegitus* males are longitudinally furrowed on the posterior sides (Fig. 1C,D). This furrow terminates in a circular depression distally, bearing a tuft of setae which projects mesad (Fig. 1C, D) as also described and illustrated by Chamberlin (1917, p. 252, plate 6, fig. 6). This modification was added to the description of character 54 to accommodate this species.

The morphological character matrix was compiled using Mesquite v.3.4 (Maddison and Maddison, 2018) and is provided as an annotated NEXUS-file (Supplement 3; http://morphobank.org/permalink/?P3757).

Images were processed with Adobe Photoshop CS6 and figures assembled in Adobe InDesign CS6. Terminology and abbreviations for the peristomatic structures, mandibles and first maxillae follow Ganske et al. (2018a,b) and references therein.

Phylogenetic analyses

Molecular data analyses. Sequence alignments were done using Muscle (Edgar, 2004; retrieved from the EMBL-EBI webpage: www.ebi.ac.uk/Tools/msa/muscle/) and Mafft (v.7, Katoh et al., 2017; retrieved from https://mafft.cbrc.jp/alignment/server/), both with default settings. For the 18S rRNA and 16S rRNA multiple sequence alignments, the endings were trimmed after alignment with Mafft/Muscle. Poorly aligned regions of the 18S rRNA and 28S rRNA sequences were discarded using Gblocks v.0.91b (Talavera and Castresana, 2007) with all options for a less stringent selection that allow smaller final blocks, gap positions within final blocks and less strict flanking positions (results are listed in Table 2). Resulting alignments were visualized with PhyDE® 0.9971 (J. Müller, K. Müller, C. Neinhuis, D. Quandt). The final alignment files (using Mafft, Muscle and Gblocks) used for the phylogenetic and genetic distance analyses are provided as NEXUS-files (Supplement 4).

Multiple sequence alignments were concatenated using SequenceMatrix (Vaidya et al., 2011) and exported as PHYLIP-files. Three molecular partitions were analysed independently: (i) 18S rRNA + 28S rRNA, (ii) 16S rRNA + COI, (iii) 18S rRNA + 28S rRNA + 16S rRNA + COI. Missing sequences were scored as unknown.

Maximum-likelihood analysis was performed using RAxML v.8.2.10 (Stamatakis, 2014) on XSEDE (Towns et al., 2014) within the CIPRES Science

Table 2
Positions removed by Gblocks with less stringent options allowing smaller final blocks, gap positions within final blocks and less strict flanking positions for the 18S rRNA and 28S rRNA multiple sequence alignments

Loci	Number of positions					
	Original alignment		Gblocks alignment		% removed	
	Mafft	Muscle	Mafft	Muscle	Mafft	Mafft
18S	2261	2261	1755	1752	23	23
28S	382	391	329	329	14	16

Gateway (Miller et al., 2010). The unique general time-reversible (GTR) model of sequence evolution was used (RAxML implements only GTR-based models of nucleotide substitutions) together with rapid bootstrap algorithm with 1000 iterations to estimate nodal support (other parameters were set as the defaults). All resulting ML trees are provided as NEXUS-files together with the corresponding in-/output-files from the ML analyses (Supplement 5).

The trees were visualized and edited using FigTree v.1.4.2 (http://tree.bio.ed.ac.uk/software/figtree/) and Dendroscope v.3.5.10 (Huson and Scornavacca, 2012) and finally adjusted in Adobe Illustrator CS6.

Pairwise, within-group and between-group mean distances were estimated using Mega7 (v.7.0.26, Kumar et al., 2016) with the Muscle + GBLOCKS aligned datasets for 18S rRNA and 28S rRNA and the Muscle aligned datasets for 16S rRNA and COI. Groups were defined as follow: (i) subgenus *Lithobius*, (ii) subgenus *Monotarsobius*, (iii) subgenus *Sigibius*, (iv) Lithobiidae, non-*Lithobius*, and (v) Henicopidae. P-distance was used as a substitution model including transitions and transversions. Indels and missing data were treated using pairwise deletion. The results are shown in Supplement 6.

Morphological data analyses. Parsimony analyses under equal weights and implied weights (k = 1–23) using TNT v.1.5 (Dec. 2017) (Goloboff and Catalano, 2016) follow Ganske et al. (2018a), using Traditional heuristic searches. All resulting parsimony trees are attached as TREE-files together with the corresponding input-/output-files from the parsimony analyses (Supplement 7).

Combined analyses (morphological and molecular data). The morphological and the molecular data (Muscle + Gblocks aligned) were combined in one file for parsimony analyses using TNT v.1.5 (Dec. 2017) (Goloboff and Catalano, 2016) and BI analysis using MrBayes v.3.2.71 (Huelsenbeck and Ronquist, 2001; Ronquist and Huelsenbeck, 2003). For parsimony analyses, the analytical parameters follow Ganske et al. (2018a) except for estimating the Bremer support values. They were calculated while doing heuristic searches under equal weights with defined constraints. Constraints were defined while marking a clade nonmonophyletic from any of the most parsimonious trees. The difference between the retrieved tree length and the original shortest tree length equals the Bremer support value for this node. This procedure was repeated for all nodes. All resulting parsimony trees are attached as TREE-files together with the corresponding input-/output-files from the analyses (Supplement 8).

Bayesian analysis was performed with a mixed dataset (Muscle + Gblocks aligned) applying the GTR substitution model with gamma-distributed rate variation across sites and a proportion of invariable sites for the sequence data and gamma-shaped rate variation for the morphological data. The analysis was run with 10 000 000 generations sampling trees every 500 generations. Eight Markov chains per run were carried out in two independent runs and a relative burnin of 25% was used. Convergence of chains was determined according to the average standard deviation (below 0.05) and potential scale reduction factor (PSRF) around 1.0. A 50% majority rule consensus tree with posterior probabilities was retrieved (see Supplement 13). All resulting Bayesian trees are attached as TREE-files together with the corresponding input-/output-files from the analysis (Supplement 13).

Morphological character tracing and optimization. Morphological characters were mapped on the total evidence tree based on 18S rRNA + 28S rRNA + 16S rRNA + COI + morphology (parsimony, TNT) and previously aligned with Muscle using the software Mesquite v.3.40 (Maddison and Maddison, 2018). To evaluate the evolution of those characters, the ancestral state reconstruction used parsimony. On one of the two most parsimonious trees based on 18S rRNA + 28S rRNA + 16S rRNA + COI + morphology and aligned with Muscle, character optimizations (unambiguous changes only) were examined using ASADO v.1.61 (Nixon, 2004).

Supplements 1–2 and 4–13 are available using the following link https://doi.org/10.6084/m9.figshare.c.5022182.

Results

Molecular data analyses

Pairwise, within-group and between-group mean distances for all genes are given in Supplement 6 and are briefly evaluated in the following. The log likelihoods of the ML trees for each of the three partitions aligned with Mafft and Muscle are presented in Table 3. For all partitions, the highest log likelihood was calculated for the Muscle alignment. The following discussion refers to the ML trees achieved from the Muscle (always on the left in Figs 5–7, 9) and the Mafft (always on the right in Figs 5–7, 9) multiple sequence alignments for comparison and to find consistently supported or conflicting hypotheses (see also Supplement 5).

18S rRNA + 28S rRNA. The average genetic distance for all 41 species belonging to the genus

Table 3
Log likelihoods of the ML trees for the three molecular partitions and shortest tree lengths for most parsimonious trees using molecular and morphological data in combination previously aligned with MAFFT and MUSCLE

	Alignment algorithm	
Dataset	MAFFT	MUSCLE
18S + 28S	−8978.778384	***−8565.605403***
16S + COI	−23784.724004	***−23502.414805***
18S + 28S+16S + COI	−34221.980881	***−33467.736341***
18S + 28S+16S + COI + morpho	7688	***7530***

Italic-bold numbers indicate highest log likelihood and shortest tree length. 18S, 18S rRNA dataset; 16S, 16S rRNA dataset; 28S, 28S rRNA dataset; COI, COI dataset; morpho, morphological dataset.

Lithobius, with available 18S rRNA sequences, is 1.3% and for all species assigned to the subgenera *Lithobius*, *Monotarsobius* and *Sigibius* is 0.6%, 2.0% and 5.4%, respectively (Supplement 6, Fig. 5). Comparing the between-group mean distances for species of *Lithobius*, the subgenus *Sigibius* shows the highest distances to all other subgenera (3.5–4.3%). The within-group mean distance of Henicopidae is 7.9% and for all other sampled Lithobiidae (*Lithobius* excluded) 1%.

The average genetic distance for all 43 species belonging to the genus *Lithobius*, with available 28S rRNA sequences, is 8.0% and for all species assigned to the subgenera *Lithobius*, *Monotarsobius* and *Sigibius* is 1.7%, 27.2% and 45.9% respectively. Comparing the between-group mean distances for species of *Lithobius*, the subgenus *Sigibius* shows the highest distances to all other subgenera (24.4–32.2%). The within-group mean distance of Henicopidae is 67.5% and for all other sampled Lithobiidae (*Lithobius* excluded) 3.1%.

The sequenced fragment of the 18S rRNA is rather conservative (1327 conserved sites) and only contains 185 parsimony-informative sites along the strand with 1759 bases for the whole dataset. The parsimony-informative sites further reduce to 67 if only sequences of Lithobiidae are considered (1490 conserved sites). The 28S rRNA dataset provides 275 parsimony-informative sites throughout the whole dataset including Henicopidae and the outgroup (31 conserved sites; strand of 326 bases). Within Lithobiidae, there are 92 parsimony-informative sites (67 conserved sites).

Based on the ML analyses using the nuclear ribosomal genes, monophyly of Lithobiidae is contradicted in the MUSCLE tree by *Lithobius holsti* grouping (with weak support) with Henicopidae. By contrast, both lithobiomorph families are monophyletic in the MAFFT tree. In both trees Ethopolyinae is paraphyletic. Bootstrap support values > 80% in both trees were estimated only for *L. giganteus* + *D. loricatus*, *L. atkinsoni* + *L. peregrinus*, and *L. variegatus* + *L. rubriceps* **stat.n.** as well as a group consisting of *L. agilis*, *L. erythrocephalus*, *L. schuleri*, *L. stygius*, *L. atkinsoni* and *L. peregrinus*. The subgenus *Lithobius* is polyphyletic, composed of two clades, one with *L. castaneus* + *L. pilicornis* and the other uniting more than 30 predominantly European species.

16S rRNA + COI. The average genetic distance for all 41 species belonging to the genus *Lithobius*, with available 16S rRNA sequences, is 21.8% and for all species assigned to the subgenera *Lithobius*, *Monotarsobius* and *Sigibius* is 21.4%, 21.2% and 23.7%, respectively (Supplement 6, Fig. 6). Comparing the between-group mean distances for species of *Lithobius*, the subgenera *Sigibius* and *Monotarsobius* show the highest distance to each other, with 22.9%. The within-group mean distance of Henicopidae is 20.8% and for all other sampled Lithobiidae (*Lithobius* excluded) 23.5%.

The average genetic distance for all 30 species belonging to the genus *Lithobius*, with available COI sequences, is 19.6% and for all species assigned to the subgenera *Lithobius*, *Monotarsobius* and *Sigibius* is 17.8%, 32.0% and 16.7%, respectively. Comparing the between-group mean distances for species of *Lithobius*, the subgenera *Sigibius* and *Lithobius* show the highest distance to each other with 24.8%. The within-group mean distance of Henicopidae is 19.5% and for all other sampled Lithobiidae (*Lithobius* excluded) 20.6%.

The sequenced fragment of the 16S rRNA shows 308 parsimony-informative sites (179 conserved sites) along the strand with 541 bases for the whole dataset. The parsimony-informative sites reduce to 275 if only sequences of Lithobiidae are considered (198 conserved sites). The COI dataset provides 304 parsimony-informative sites throughout the whole dataset including Henicopidae and the outgroup (227 conserved sites; strand of 676 bases). Within Lithobiidae, 290 sites are parsimony-informative (238 conserved sites).

The simultaneous analyses for the 16S rRNA and COI genes resolve Henicopidae and Lithobiidae as reciprocally monophyletic sister groups, and the genus *Australobius* as sister taxon to all other sampled Lithobiidae (bootstrap for all Lithobiidae exclusive of *Australobius*: MUSCLE 98%, MAFFT 99%). The subfamily Ethopolyinae, the genus *Lithobius*, and the subgenera *Lithobius*, *Monotarsobius* and *Sigibius* are resolved as nonmonophyletic. Some shallower nodes within the genus *Lithobius* are strongly supported in both ML trees, for example *L. pilicornis* + *L. castaneus* (MUSCLE 96%, MAFFT 93%) and *L. tricuspis* + *L. piceus* (both 100%), *L. viriatus* + (*L. peregrinus* + *L. atkinsoni*) (both 100% for each node), *L. giganteus* + *D. loricatus* (MUSCLE 99%, MAFFT 100%), *L. lucifugus* + *L. lusitanus* (both 99%), *L. crassipes* + *L. crassipesoides*

(MUSCLE 99%, MAFFT 95%), and *L. aeruginosus* + *L. austriacus* (MUSCLE 73%, MAFFT 78%). A clade consisting of *L. tenebrosus* as sister group to *L. setiger* **stat.n.** + (*L. cyrtopus* + *L. pelidnus*) finds 92% (MUSCLE) and 94% (MAFFT) bootstrap support. *L. glacialis* is resolved as sister group to *L. muticus* + (*L. latro* + *L. mutabilis*) supported by 59% (MUSCLE) and 61% (MAFFT) bootstrap values and the internal relationships receive high bootstrap values in both trees. The analyses based on the mitochondrial markers recover a clade consisting of *L. lapidicola*, *L. melanops*, *L. borealis*, *L. lucifugus*, *L. lusitanus*, *L. piceus*, *L. tricuspis*, *L. agilis*, *L. erythrocephalus*, *L. microps*, *L. schuleri*, *L. viriatus*, *L. atkinsoni* and *L. peregrinus* (MUSCLE 96%, MAFFT 97%).

18S rRNA + 28S rRNA + 16S rRNA + COI. In the MUSCLE/MAFFT trees of the simultaneous analysis of the four loci, 32/36 nodes, respectively, out of 57 nodes are supported with bootstrap values >50% (and of those 24/23 nodes, respectively, are >80%) (Fig. 7). The analyses of all sequence data support the relationship of Henicopidae and Lithobiidae as sister taxa and reciprocally monophyletic. The genus *Australobius* is the sister taxon to all other sampled Lithobiidae with a bootstrap support value of 97% for the latter node in both trees. Nonmonophyly is resolved for the subfamily Ethopolyinae, the genus *Lithobius*, and the subgenera *Lithobius*, *Monotarsobius* and *Sigibius*.

A clade including all species of the genus *Lithobius* together with other representatives of the subfamily Lithobiinae (*Sozibius* and *Harpolithobius*) as well as the subfamilies Gosibiinae (*Arenobius*) and Pterygoterginae (*Disphaerobius*) is supported with 95% (MUSCLE) and 90% (MAFFT). The positions and relationships of the lithobiine *S. tuobukus* and the gosibiine *A. manegitus* within this clade are not well supported in either tree, whereas a close relationship of the pterygotergine *D. loricatus* with *L. giganteus* receives high support values using both alignment strategies (99%, respectively).

The species pairs *L. pilicornis* + *L. castaneus* (MUSCLE 88%, MAFFT 79%) and *L. crassipes* + *L. crassipesoides* (MUSCLE 98%, MAFFT 96%) are resolved as sister taxa in the combined molecular analyses, which is congruent to the analytical outputs using either of the two other molecular partitions on its own (Figs 5 and 6).

A close relationship of *L. aeruginosus* and *L. austriacus* is resolved with high bootstrap values in the ML trees using all molecular sequences together (MUSCLE 92%, MAFFT 96%) and 16S rRNA + COI sequences (MUSCLE 73%, MAFFT 78%, Fig. 6).

The hypothesis uniting *L. tenebrosus* as the sister taxon to *L. setiger* **stat.n.** + (*L. cyrtopus* + *L. pelidnus*) resolved by the combined 16S rRNA + COI data (Fig. 6) finds additional support from the simultaneous analyses using all molecular markers (MUSCLE 95%, MAFFT 97%).

The simultaneous analyses (18S rRNA + 28S rRNA + 16S rRNA + COI) recover a clade consisting of *L. lapidicola*, *L. melanops*, *L. borealis*, *L. lucifugus*, *L. lusitanus*, *L. piceus*, *L. tricuspis*, *L. agilis*, *L. erythrocephalus*, *L. microps*, *L. schuleri*, *L. stygius*, *L. viriatus*, *L. atkinsoni* and *L. peregrinus* (MUSCLE 89%, MAFFT 92%). Some internal nodes of this clade have high bootstrap support values, for example a clade with *L. lapidicola* + (*L. melanops* + (*L. borealis* + (*L. lusitanus* + *L. lucifugus*))), which is also supported using the mitochondrial 16S rRNA + COI data (Fig. 6).

A clade consisting of *L. glacialis* as sister group to *L. muticus* + (*L. mutabilis* + *L. latro*), recovered by the simultaneous analyses using all molecular sequences (MUSCLE 55%, MAFFT 62%), also was found in the 16S rRNA + COI analyses (MUSCLE 59%, MAFFT 61%, Fig. 6). The internal nodes of this group are strongly supported with >90%.

Lithobius variegatus and *L. rubriceps* **stat.n.** are hypothesized to be sister taxa in both trees, but do not receive high bootstrap support. Although this close relationship is strongly supported by the analyses based on the nuclear ribosomal markers (Fig. 5), the mitochondrial data suggest a close but nonsister group relationship of the two species (Fig. 6).

Differences between the two trees include the sister taxon of *L. giganteus* + *D. loricatus*, which is either *L. curtipes* (MAFFT) or *L. holstii* (MUSCLE). Furthermore, the positions of some species or species groups are not consistently resolved in both trees, for example *L. agilis*, *L. erythrocephalus*, *L. stygius* (28S rRNA sequence only), *L. nodulipes* + *L. dentatus*, *L. pygmaeus* + *L. macilentus*, and *L. validus* + (*L. variegatus* + *L. rubriceps* **stat.n.**).

Morphological information

New morphological data (peristomatic structures, mandibles and first maxillae). We obtained new information from the peristomatic structures, mandibles and first maxillae from sixteen species, namely *A. manegitus*, *S. tuobukus*, *L. atkinsoni*, *L. borealis*, *L. glacialis*, *L. lusitanus*, *L. melanops*, *L. pilicornis*, *L. pygmaeus*, *L. schuleri*, *L. silvivagus*, *L. stygius*, *L. setiger* **stat.n.**, *L. viriatus*, *L. crassipesoides* and *L. carinthiacus* (see Supplement 2) now included in the morphological character matrix (Supplement 3). The general structure of the epipharynx, hypopharynx, mandibles and first maxillae for the newly studied species is congruent with the observations and descriptions provided by Ganske

et al. (2018a,b). In the following, we describe and illustrate our new observations:

1. *L. borealis*, epipharynx, number of transverse bulge(s) at border between labral and clypeal parts of epipharynx: two bulges (bud – distal transverse bulge, bup – proximal transverse bulge) in contrast to one bulge, e.g. *L. crassipesoides* (compare Fig. 2A,B & C). This state was hitherto only observed for *L. calcaratus*, *L. lucifugus* and *L. tenebrosus* (Ganske et al., 2018b, fig. 3C).
2. *L. viriatus* and *L. atkinsoni*, epipharynx, lateral expansion of median sensilla cluster (msc): the median sensilla cluster partly overlaps with the lateral spine fields (lsp): observed for the first time in species assigned to the subgenus *Lithobius* in contrast to an isolated median sensilla cluster, e.g. *L. borealis* (compare Fig. 2D, E & F–H; see also Ganske et al., 2018b, fig. 10A–D for comparison).
3. *L. atkinsoni*, hypopharynx, hypopharyngeal spine field (hsp): low number of vestigial hypopharyngeal spines in contrast to a high number of well-developed spines in other Lithobiidae, e.g. *A. manegitus* (compare Fig. 3A, B, C & D; see also Ganske et al., 2018b, fig. 13 for comparison).
4. *L. pilicornis*, mandibles, spinulation on the internal side of the margin to mandibular teeth: bilaterally branching bristles expanding along all four mandibular teeth in contrast to spines/bristles along the ventralmost tooth or maximum second ventralmost teeth only, e.g. *L. setiger* **stat.n.** (compare Fig. 4A, B, C & D; see also Ganske et al., 2018a, figs 8 and 9 for comparison).

Morphological data analyses. The parsimony analysis of 59 species based on the matrix with 61 morphological characters weighted equally resulted in 4302 shortest cladograms of 298 steps (consistency index 0.204, retention index 0.307) (Fig. 8). Henicopidae is resolved as paraphyletic, placing Anopsobiinae s.s. (*A. neozelanicus* and *D. flavens*) as sister group to Lithobiidae in the strict consensus tree. A node resolving Lithobiidae as monophyletic does not receive high Jackknife frequencies or Bremer support values. The genus *Lithobius* and its subgenera *Lithobius* and *Monotarsobius* are resolved as nonmonophyletic. The subgenus *Sigibius* clusters with *L. aeruginosus* + *L. austriacus* in an unresolved polytomy. Jackknife frequencies >50% are recovered only for a clade of the two sampled *Eupolybothrus*-species (86%; Bremer 3) and *L. giganteus* + *D. loricatus* (96%, Bremer 6).

Combined analyses (morphological and molecular data; Fig. 9, Supplement 13)

In the parsimony analysis, two shortest cladograms of 7530 steps were obtained under equal weights (consistency index 0.277, retention index 0.375) using the morphological matrix with 61 characters and the 18S rRNA, 28S rRNA, 16S rRNA and COI sequences aligned with MUSCLE (Table 3, Supplement 8). The same molecular data previously aligned with MAFFT plus the morphological data resulted in six shortest cladograms of 7688 steps under equal weights (consistency index 0.282, retention index 0.380) (Table 3, Supplement 8). As the parsimony trees and the Bayesian Inference tree are largely congruent, only conflicting nodes are noted here.

Of 56 nodes, 20 (MUSCLE) and 21 (MAFFT) nodes receive Jackknife support values >50%. Monophyly of both Henicopidae and Lithobiidae is supported, the latter with 100% Jackknife frequency and Bremer support of 20 in both trees. *Australobius scabrior* as sister taxon to all other Lithobiidae receives high support values (MUSCLE: 89% Jackknife, 12 Bremer; MAFFT: 68%/12 for the non-*Australobius* clade). Ethopolyinae is paraphyletic in the MUSCLE tree and the BI tree, which is not consistently resolved in the MAFFT tree. The genus *Lithobius* and its subgenera *Lithobius*, *Sigibius* and *Monotarsobius* are all resolved as polyphyletic.

A monophyletic group of *E. grossipes* + *E. fasciatus* has Bremer support of 24 (MUSCLE) and 34 (MAFFT) and receives 100% (both trees) support after Jackknife resampling. *L. crassipesoides* + *L. crassipes* (MUSCLE: 95%/17; MAFFT: 91%/14), *L. giganteus* + *D. loricatus* (MUSCLE: 99%/23; MAFFT: 99%/24), *L. pilicornis* + *L. castaneus* (MUSCLE: 88%/8; MAFFT: 61%/3; but see BI tree with *L. pilicornis* resolved as sister taxon to *L. castaneus* + *S. tuobukus* (posterior probabilities of 0.96 and 0.95)), *L. tricuspis* + *L. piceus* (MUSCLE: 99%/8, MAFFT: 100%/10), *L. austriacus* + *L. aeruginosus* (MUSCLE: 91%/11; MAFFT: 92%/10), and *L. mutabilis* + *L. latro* (MUSCLE: 94%/5; MAFFT: 92%/8) are strongly supported species pairs which were also resolved in the simultaneous analyses (see Fig. 6). A clade consisting of *L. lapidicola* + (*L. melanops* + (*L. borealis* + (*L. lusitanus* + *L. lucifugus*))) (MUSCLE: 66–99%/4–10; MAFFT: 82–99%/7–11) is further supported in the simultaneous analyses (see Fig. 6).

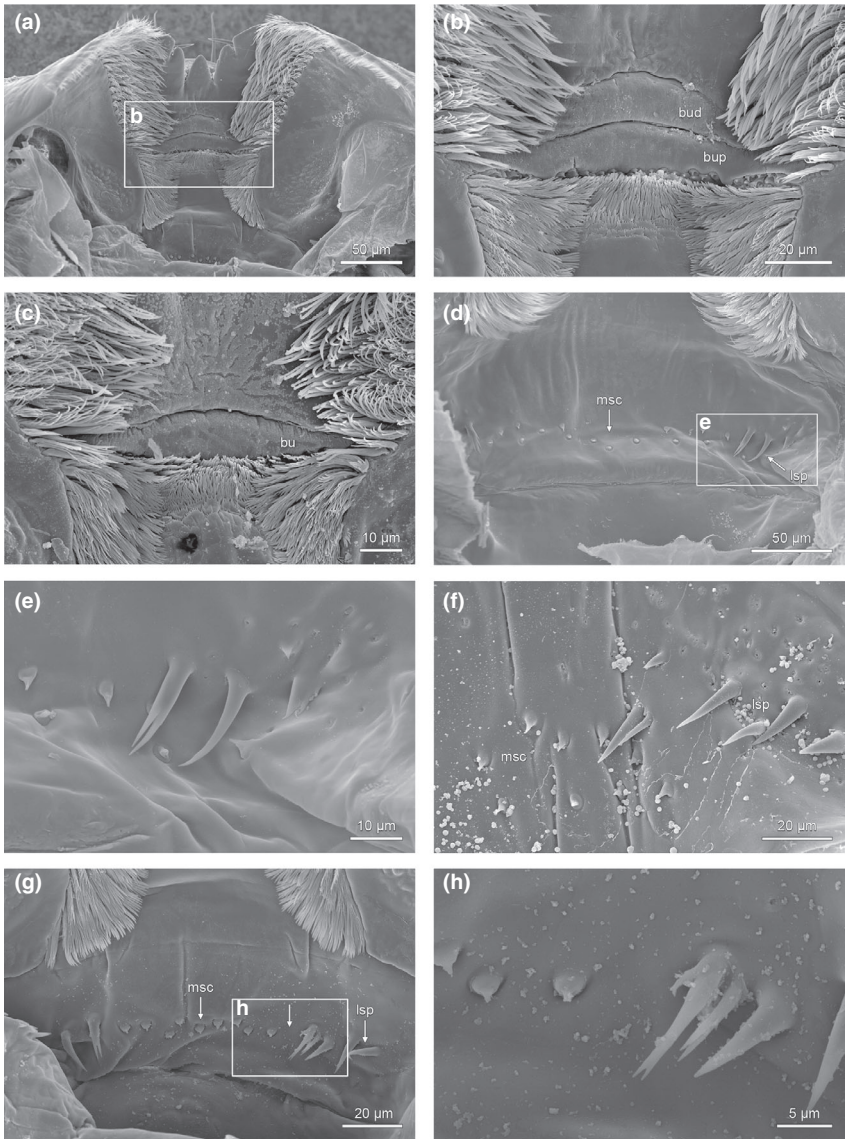

Fig. 2. Scanning electron microscopy photographs of the epipharynx and epipharyngeal structures of *Lithobius* (*Lithobius*) *borealis* (a, b, g, h) and *Lithobius* (*Lithobius*) *viriatus* (d, e): (a) Epipharynx, posterior view (top is ventral); (b) two transverse bulges (bud – distal transverse bulge, bup – proximal transverse bulge); (c) *Lithobius* (*Lithobius*) *crassipesoides*, one transverse bulge (bu); (d) clypeal part with median sensilla cluster (msc) which overlaps partly with the lateral spine field (lsp); (e) detail of (d). (f) *Lithobius* (*Lithobius*) *atkinsoni*, median sensilla cluster (msc) overlaps partly with the lateral spine field (lsp). (g) clypeal part with median sensilla cluster (msp) which is isolated (arrow) from the lateral spine field (lsp); (h) detail of (g).

Lithobius muticus resolved as sister group to *L. mutabilis* + *L. latro* is supported in the MUSCLE tree, but not in the MAFFT tree or in the BI tree. Some species are not resolved consistently and their position deviates between the trees, for example *S. tuobukus*, *A. manegitus*, *L. microps*, *L. holstii* and *L. curtipes*.

Character evolution

Results of the tracing of all morphological characters on the total evidence tree are shown in a NEXUS-file (Supplement 9) where every character can be visualized separately. Optimizations of morphological characters are depicted in Fig. 10. Selected characters are further explained in the discussion section.

Discussion

The current study provides (i) a first phylogeny of a subset of species assigned to the centipede family Lithobiidae including the subfamilies Lithobiinae, Gosibiinae, Pterygoterginae and Ethopolyinae. The study (ii) provides novel insights into the phylogenetic

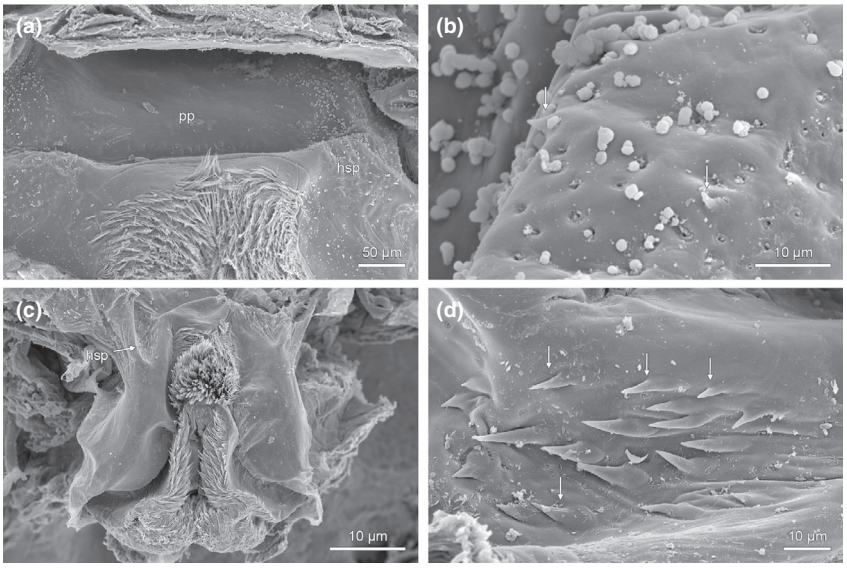

Fig. 3. Scanning electron microscopy photographs of the hypopharynx with details of hypopharyngeal spine field of Lithobiidae. (a, b) *Lithobius* (*Lithobius*) *atkinsoni*, (a) pharyngeal plate (pp) with hypopharyngeal spine field (hsp); (b) detail of (a) showing a few and vestigial hypopharyngeal spines (arrows). (c, d) *Arenobius manegitus*, (c) hypopharynx with hypopharyngeal spine field (hsp); (d) detail of (c) showing a high number and well-developed hypopharyngeal spines (arrows).

position of the lithobiine genus *Australobius*. It further highlights (iii) a mix of well supported clades and inconsistent groupings of species of the genus *Lithobius*, which are either clarified in the present study or should be further re-evaluated in subsequent projects. Additionally, it provides (iv) a brief evaluation on the phylogenetic information of the different datasets as well as different multiple sequence alignment methods. (v) Several taxonomic changes also are presented to clarify the systematic position of some taxa and update their nomenclature in accordance with the present findings.

New findings regarding the phylogeny of Lithobiidae and its subfamilies

Australobius: *sister taxon to all other Lithobiidae included in the present research*. The lithobiid *Australobius scabrior* is resolved as sister taxon to all other investigated Lithobiidae, with high support values using molecular data (simultaneous analysis; Fig. 7) and with moderate support in the combined analyses with morphology (Fig. 9). It is recovered with especially strong support by the two mitochondrial markers in combination (Fig. 6). This sister-group relationship was not resolved in previous phylogenetic studies based on morphological data only, where *A. scabrior* was deeply nested within the Lithobiidae (Koch and Edgecombe, 2008; Ganske et al., 2018a). In the current parsimony analyses based on morphology, the shortest trees recover *Australobius* in different positions within Lithobiidae, but none resolves it as sister group to all other sampled lithobiids as found in the molecular and combined analyses. However, the results of the present research are strongly supported by previous studies using the same molecular markers (e.g. Edgecombe and Giribet, 2002, fig. 6.5; Murienne et al., 2010, fig. 1; Qiao et al., 2018, fig. 3), and none of the conflicting nodes in the morphological trees is well supported. A few morphological characters are potentially informative for excluding *Australobius* from deep nodes that unite other lithobiids. These include character 4, which refers to the position of the Tömösváry organ below the inferior row of ocelli (state 2), to our knowledge unique in *Australobius* (Edgecombe and Hollington, 2002, figs 3C,E & 5) in contrast to all other Lithobiidae, in which the Tömösváry organ is anteroventral to the ocellar cluster (state 0; Fig. 10, Supplement 9). In Henicopidae the Tömösváry organ is positioned on the cephalic pleurite on the ventral side of the head (state 1; Edgecombe and Giribet, 2004), this different character state in the sister group requiring character polarity for Lithobiidae to be inferred based on the distantly allied Scutigeromorpha. Character optimization on the total evidence tree suggests that numbers of rows of bottle-shaped glandular shafts between the clypeal and labral parts of the epipharynx (character 17), although homoplastic, are congruent with early branching of *Australobius* within Lithobiidae. The nonlateral position of the porodont relative to the coxosternal teeth is another morphological character typical for the genus *Australobius* (Eason, 1996; Edgecombe and Hollington, 2002; fig. 6H) and differs in comparison to most other lithobiid species. The genus is distributed mainly in South, East and Southeast Asia, but ranges to the Seychelles and Melanesia and is the only known

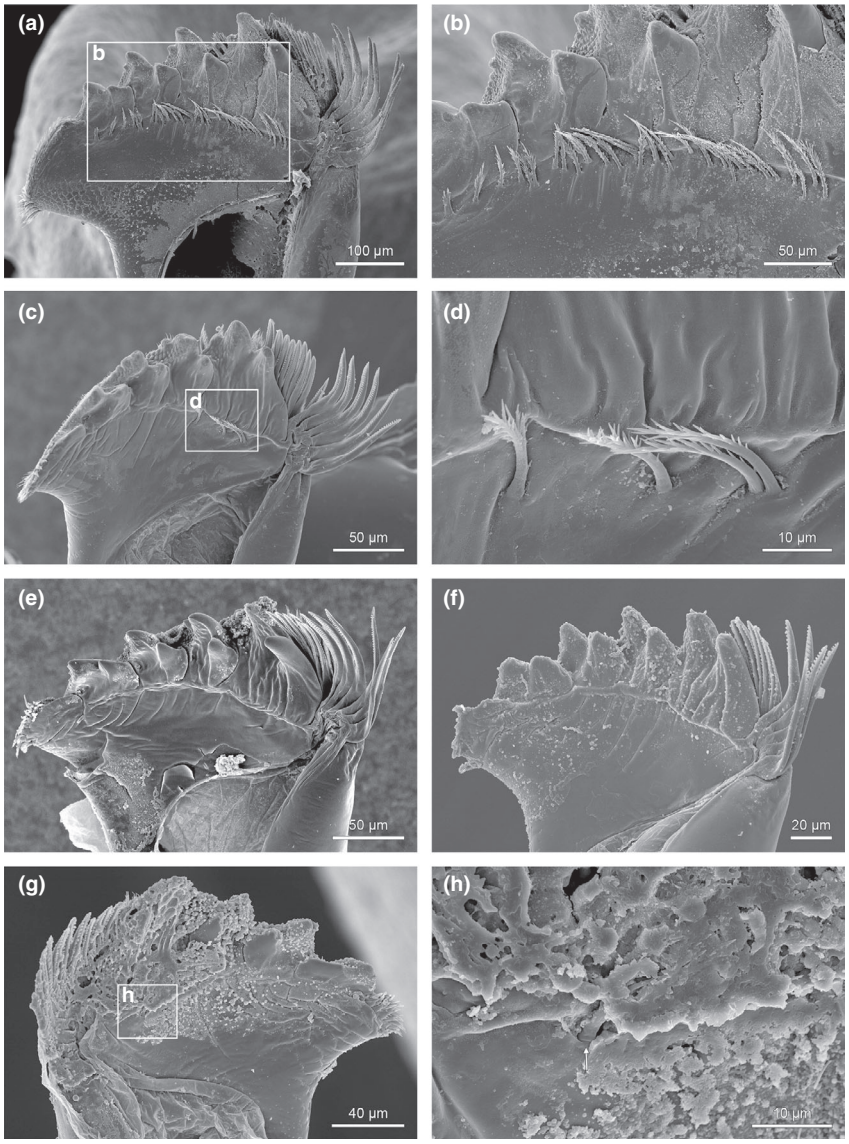

Fig. 4. Scanning electron microscopy photographs of the inner side of the mandibular gnathal edge with details of the internal spinulation of *Lithobius*. (a, b) *Lithobius* (*Lithobius*) *pilicornis,* bilaterally branching bristles expanding along all four mandibular teeth. (c, d) *Lithobius* (*Lithobius*) *setiger*, bilaterally branching bristles expanding along ventralmost tooth. (e) *Lithobius* (*Lithobius*) *tenebrosus*, no internal spinulation. (f–h) *Lithobius* (*Lithobius*) *crassipesoides*, (f) individual without internal spinulation, (g) individual with covered internal bristle and (h) detail of (g) (arrow indicates base of a densely covered but still identifiable bristle).

native lithobiid for Australia (Eason, 1978; Edgecombe and Hollington, 2002; Zapparoli and Edgecombe, 2011). The sister-group relationship between *Australobius* and other Lithobiidae may signal vicariance between lineages that are ancestrally Oriental/Australian and Palaearctic, respectively.

On the subfamily Pterygoterginae. Analyzed with morphological and molecular data or both combined, a close relationship of *L. giganteus* and the pterygotergine *D. loricatus* is consistently recovered with high support values (Figs 5-9). These taxa are each other's sister group for each analyzed partition (Figs 5-7). Thus, molecules strongly support previous morphological results (Ganske et al., 2018a,b) that the subfamily Pterygoterginae is nested within Lithobiinae. We do not have molecular data to test the morphological hypothesis that the genus *Hessebius* is closely related to this clade. The absence of a transverse bulge on the epipharynx (character 18, state 0) in both examined species is congruent with the results of the molecular phylogenetic analyses separating *giganteus* and *loricatus* from the other lithobiid species in our sample (Fig. 10, Supplement

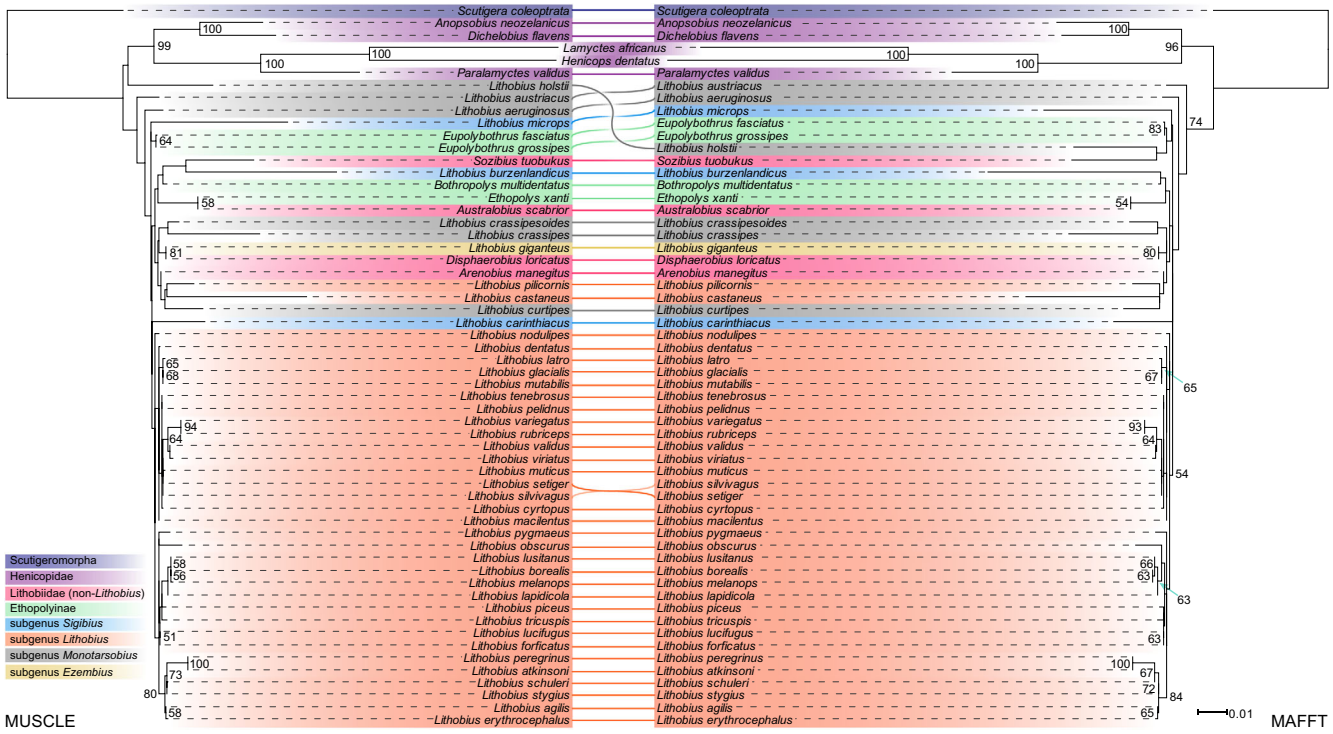

Fig. 5. Maximum-likelihood trees corresponding to the 18S rRNA + 28S rRNA data analyses with a direct comparison of the two retrieved trees using MUSCLE (left) and MAFFT (right) aligned datasets. Above nodes: bootstrap values >50%.

9). The newly obtained sequences of *D. loricatus* together with the morphological evidence is an incentive to re-evaluate the taxonomy of *Lithobius giganteus* and whether it should, instead, be considered in the genus *Disphaerobius*. Based on congruent support from morphology and molecules that Pterygoterginae is nested within Lithobiinae, such that recognizing the former contributes to paraphyly of the former, we here formally synonymize the subfamily Pterygoterginae with Lithobiinae (**syn. nov.**).

On the subfamily Ethopolyinae. Our results generally support the paraphyly of the subfamily Ethopolyinae (Figs 6–7, 10 and Fig. 9, MUSCLE only), its members forming two clades (European species of *Eupolybothrus* and North American species of *Bothropolys* + *Ethopolys*, respectively) near the base of Lithobiidae, splitting off a node crownward of *Australobius*. Although Murienne et al. (2010, fig. 1) recovered weak support for a monophyletic Ethopolyinae based on four molecular markers, the paraphyly of Ethopolyinae was recovered in some trees by Ganske et al. (2018a, figs 18, 21) based on morphology as well as by Edgecombe and Giribet (2004, fig. 14) based on combined analysis of morphological and molecular data. All type species for these genera are included in the present study (*Bothropolys* = *B. multidentatus; Eupolybothrus* = *E. grossipes; Ethopolys* = *E. xanthi*). Ethopolyinae is diagnosed by having numerous coxal pores scattered as a field rather than organized as a single row. Paraphyly implies either two independent gains of this character (from an ancestral state of a single row of coxal pores, shared by Henicopidae and *Australobius*) or a reversal from a field of pores to a single row. Character optimization on the total evidence tree (Fig. 10) suggests that the shape of the coxosternal dental margin (character 12) is consistent with paraphyly of Ethopolyinae. Subsequent phylogenetic studies focusing on the Ethopolyinae based on a denser taxon sampling should assist with a better understanding of its phylogenetic status.

The phylogeny of the genus Lithobius: *state of the art*

The nonmonophyly of Lithobius and its subgenera Lithobius, Monotarsobius *and* Sigibius. As stated previously by some authors (Koch and Edgecombe, 2008; Ganske et al., 2018a), the genus *Lithobius* is consistently resolved as paraphyletic or polyphyletic either with morphological or molecular approaches or when combining both (present study). The nonmonophyly of the genus is further amplified here as the sampled exemplars of the North and Central

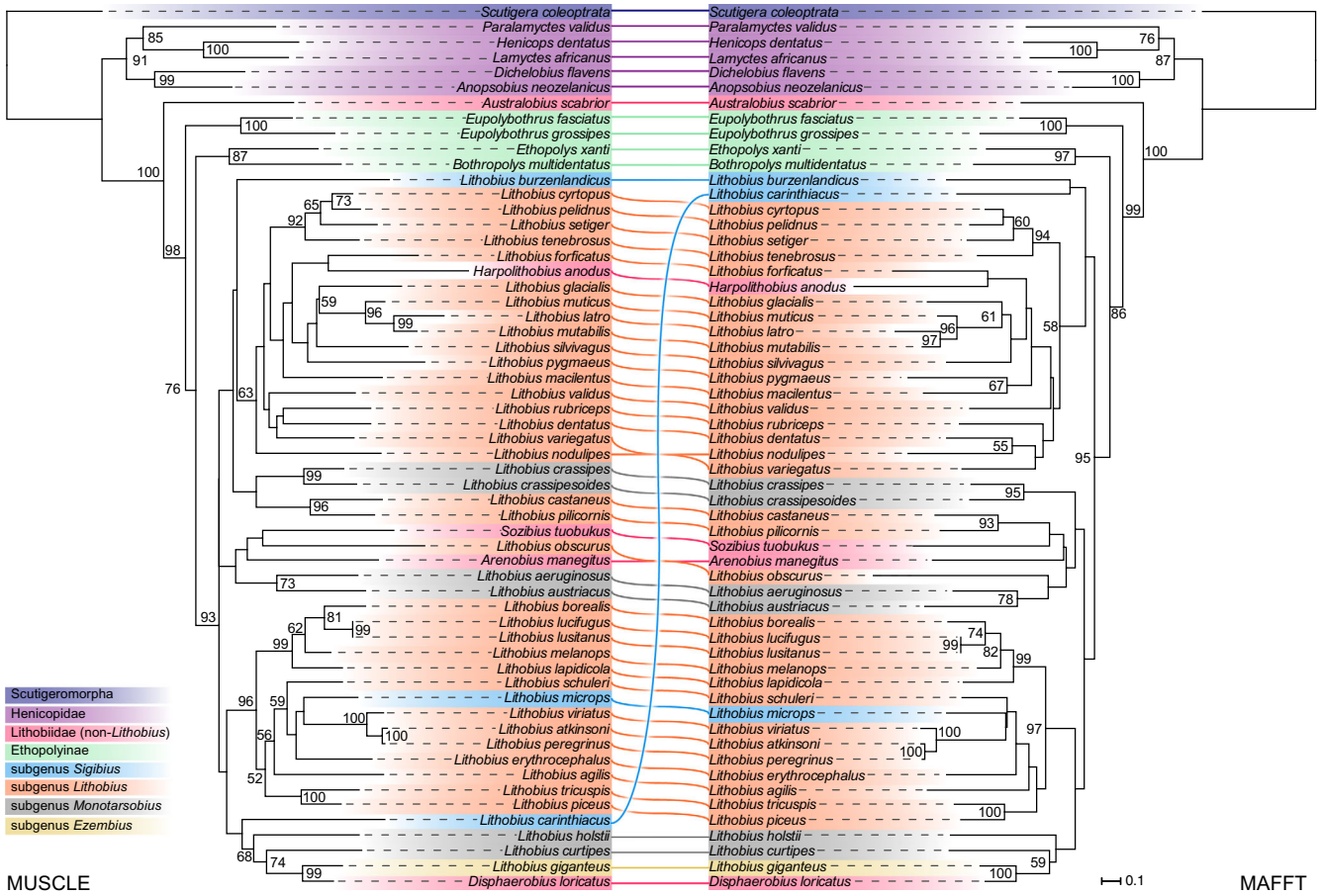

Fig. 6. Maximum-likelihood trees corresponding to the 16S rRNA + COI data analyses with a direct comparison of the two retrieved trees using the MUSCLE (left) and MAFFT (right) aligned datasets. Above nodes: bootstrap values >50%.

American genera *Sozibius* Chamberlin, 1912 and *Arenobius* Chamberlin, 1912 are positioned within *Lithobius* (Figs 5–9). *Arenobius* is hitherto classified with about other 30 North and Central American genera or subgenera in the subfamily Gosibiinae. In this respect, it is noteworthy that the sampled species *S. tuobukus* and *A. manegitus* were assigned to the genus *Lithobius* by original designation (Chamberlin, 1911). *Sozibius* is assumed to be closely related to the North American genera *Neolithobius* Stuxberg, 1875; *Nuevobius* Chamberlin, 1941; *Pholobius* Chamberlin, 1940; and *Serrobius* Causey, 1942 (regarded as a junior synonym of *Sozibius*) (Zapparoli and Edgecombe, 2011). To verify these assumed relationships, representatives of the listed genera need to be investigated on a phylogenetic basis. The position of *Arenobius* as a representative of Gosibiinae deeply nested within the genus *Lithobius* and therefore Lithobiinae, suggests a thorough consideration of its systematic position (and Gosibiinae relative to Lithobiinae more broadly). The phylogenetic position of these two endemic North American genera is not resolved consistently using different molecular markers and analytical parameters, except for the simultaneous analyses based on all genes, but receives low support values (Fig. 7). Future analyses including American and European lithobiid genera are needed to determine to what extent the American taxa form larger clades.

The subgenera *Lithobius*, *Monotarsobius* and *Sigibius* are resolved as nonmonophyletic in all molecular trees obtained from the three different partitions (Figs 5–7), the morphological (Fig. 8), and the combined molecular and morphological tree (Fig. 9). This corroborates the hypothesis previously made by Ganske et al. (2018a) based on morphology alone. Additionally, Qiao et al. (2018) included a few species assigned to the subgenera *Lithobius* and *Monotarsobius* in their COI-analysis (focusing on the identification of some *Ezembius* species), which likewise suggested they do not cluster together. The monophyly of the subgenus *Ezembius* cannot be further discussed as only the molecular data of *L.* (*E.*) *giganteus* are now available.

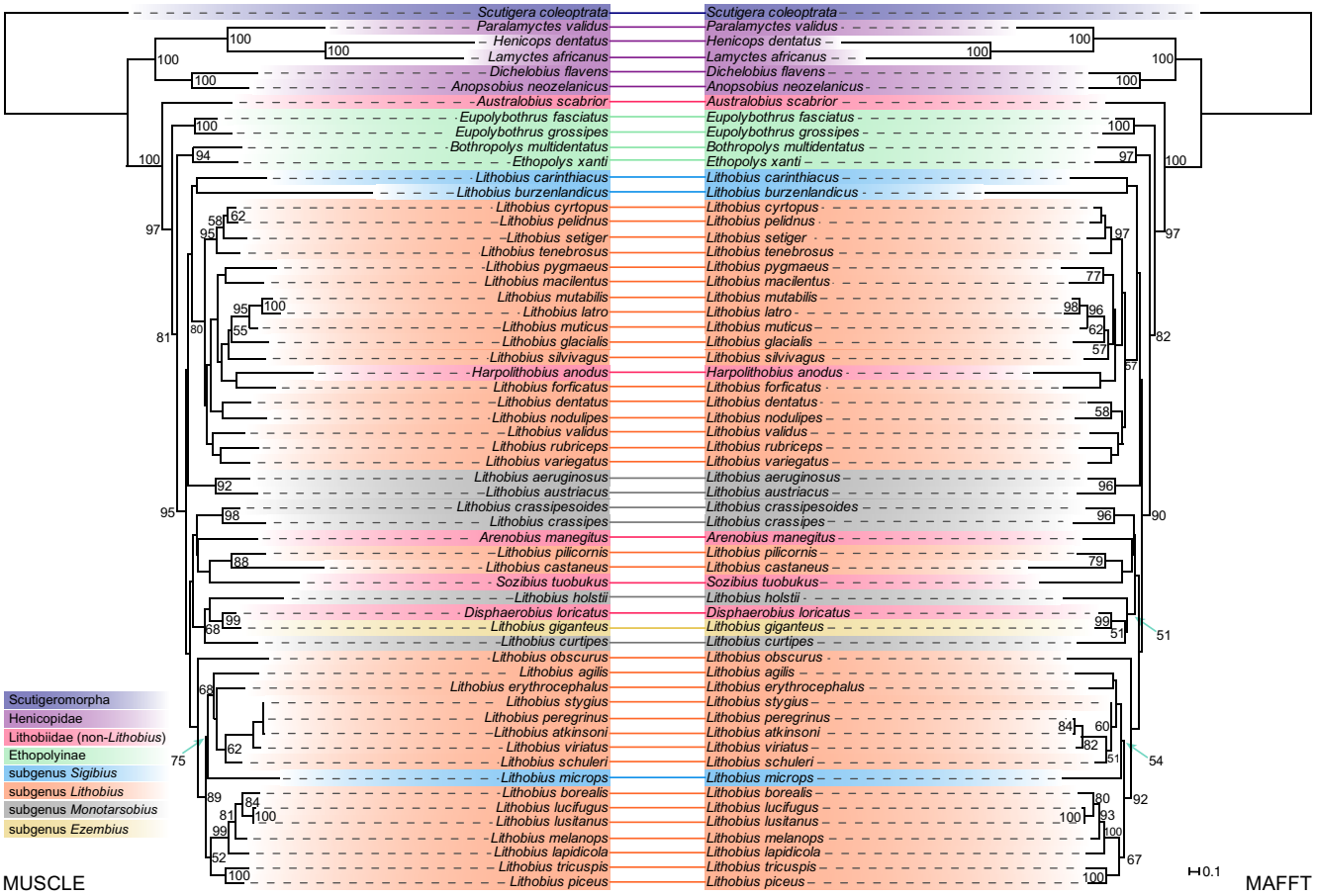

Fig. 7. Maximum-likelihood tree based on all molecular data (18S rRNA + 28S + COI + 16S) with a direct comparison of the two retrieved trees using MUSCLE (left) and MAFFT (right) aligned datasets. Above nodes: bootstrap values >50%.

The subgenus *Sigibius* has its three sampled species scattered across the tree in all molecular analyses (Figs 5–7), none of them uniting with each other, and a high within-group mean distance for the 28S rRNA sequences (45.9%) has been calculated. Weak support for their grouping is provided only by morphology, in which they unite as a clade in some but not all most parsimonious trees (MPTs; Fig. 8). From the perspective of molecular data, the diagnostic characters of this subgenus, e.g., few ocelli, lack of tergal projections, indistinct tarsal articulations (see Supplement 9, chars 37 & 40) appear to be subject to convergence, perhaps correlated with small body size.

Although the subgenus *Monotarsobius* appears polyphyletic (also high within-group mean distance for 28S rRNA sequences with 27.2%), a close relationship of *L.* (*M.*) *aeruginosus* and *L.* (*M.*) *austriacus*, hitherto highlighted by Ganske et al. (2018a), finds additional support in the present analyses using a combination of 16S rRNA + COI (Fig. 6), all genes together (Fig. 7), and in the combined analysis (Fig. 9). However, this is not supported using the concatenated 18S rRNA + 28S rRNA dataset (Fig. 5).

As our analyses indicate that each of subgenera *Lithobius*, *Sigibius* and *Monotarsobius* are polyphyletic, we suggest that they should no longer be employed in future taxonomic treatments on the group.

It is still questionable if the subgenera *Tracolithobius* Matic, 1962, *Chinobius* Verhoeff, 1934 and *Porobius* Attems, 1926 are monophyletic and if their taxonomic status is justified, and the status of the monotypic subgenus *Dacolithobius* Matic, 1961 is especially uncertain. The latter is based on *L. domogledicus* Matic, 1961, which shows striking similarities in male characters with *L. setiger* as described by Kaczmarek (1977), for example in presenting a thickened and emarginated tergite 14 equipped with numerous dark setae. This unique character calls for further investigation and perhaps detailed examination of *L. domogledicus* to further clarify the validity of the subgenus *Dacolithobius*.

On the alpine clade L. glacialis, L. latro, L. mutabilis *and* L. muticus. A clade of species including *L. glacialis* as sister taxon to *L. muticus* + (*L. latro* + *L. mutabilis*)

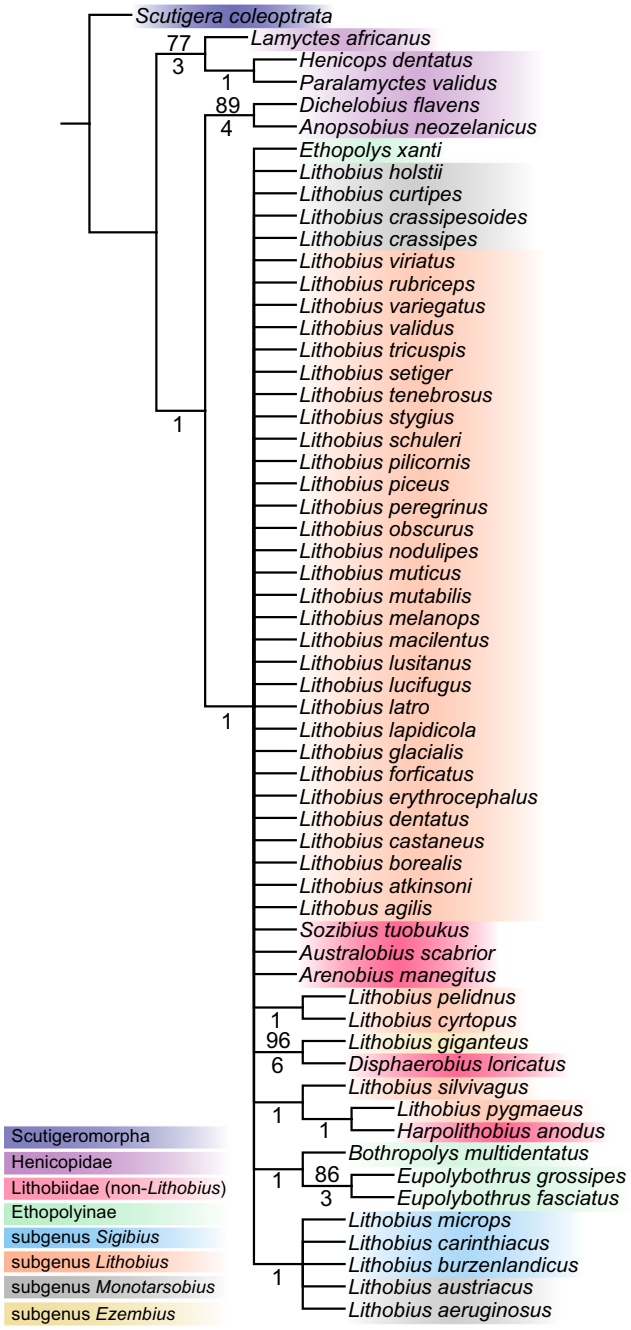

Fig. 8. Strict consensus tree of 4302 shortest cladograms of 298 steps from the parsimony analysis based on morphological data. Above nodes: Jackknife frequencies >50%, below nodes: Bremer support values.

was consistently resolved in the 16S rRNA + COI, combined molecular, and combined analyses of molecular and morphological data (not the MAFFT tree) (Figs 6, 7, 9). These are mainly alpine species (above timberline), with *L. muticus* and *L. mutabilis* also being eurytopic (Koren, 1992). The specimens of *L. glacialis* and *L. latro* used in this study were sampled at an alpine pasture edge close to a mountain peak (>1700 m above sea level (asl)), the other two in mixed forests (beech, spruce, oak, hazel) at lower altitudes (480–1000 m asl).

A close relationship of *L. glacialis* and *L. mutabilis* has been assumed earlier (Pilz et al., 2008). The two species can be distinguished based on some morphological characters (e.g. modifications on the 13th–15th legs in males, number of antennal articles, body length). As we show now, they also can be clearly separated by molecular data (pairwise distances: 16S rRNA 17.1%, COI 14.9%; Supplement 6).

Systematic considerations based on the phylogenetic analyses

Notes on Lithobius setiger. A close relationship between *L. tenebrosus tenebrosus* and the subspecies *L. tenebrosus setiger* is resolved in all of the obtained molecular trees (Figs 5–7). Here, it is usually hypothesized that *L. tenebrosus* is sister taxon to a clade including *L. setiger*, *L. pelidnus* and *L. cyrtopus* (Figs 6 and 7). Only the combined analysis using MUSCLE relates *L. setiger* as sister taxon to a clade of *L. tenebrosus*, *L. pelidnus* and *L. cyrtopus* (Fig. 9).

Kaczmarek (1977) distinguished *L. tenebrosus setiger* from *L. tenebrosus* by the presence of a thickened and emarginated tergite 14 equipped with numerous dark setae posteriorly (Fig. 2b therein). Besides this striking difference, we noted a difference in the internal spines on the mandibles (character 31), which are present in *L. tenebrosus setiger* (state 1) and absent in the nominal species (state 0; see Figs 4C–E, 10).

These differences coupled with the results of the phylogenetic analyses, and high genetic distances between *L. tenebrosus* and *L. tenebrosus setiger* (16S rRNA: 13.9%; COI: 15.9%), in comparison to the lowest calculated genetic distance of other species pairs (16S rRNA: 1.6%; COI: 0.3%) (Supplement 6), leave no doubt that *L. tenebrosus setiger* is a separate taxon from *L. tenebrosus* and should in fact be elevated to species rank, viz. *Lithobius setiger* Kaczmarek, 1977 **stat.n.**

Notes on Lithobius variegatus variegatus *and* L. variegatus rubriceps. Two subspecies *L. variegatus variegatus* and *L. variegatus rubriceps* are included in the study. The latter was described as a full species by Newport (1845) from southern Spain and it was since then thought to be similar (except in size) to *L. variegatus* Leach, 1814, hitherto considered endemic to the British Isles. Based on the study of some lithobiids from northwestern Spain, Eason and Serra (1986) recorded *L. variegatus* for the first time from

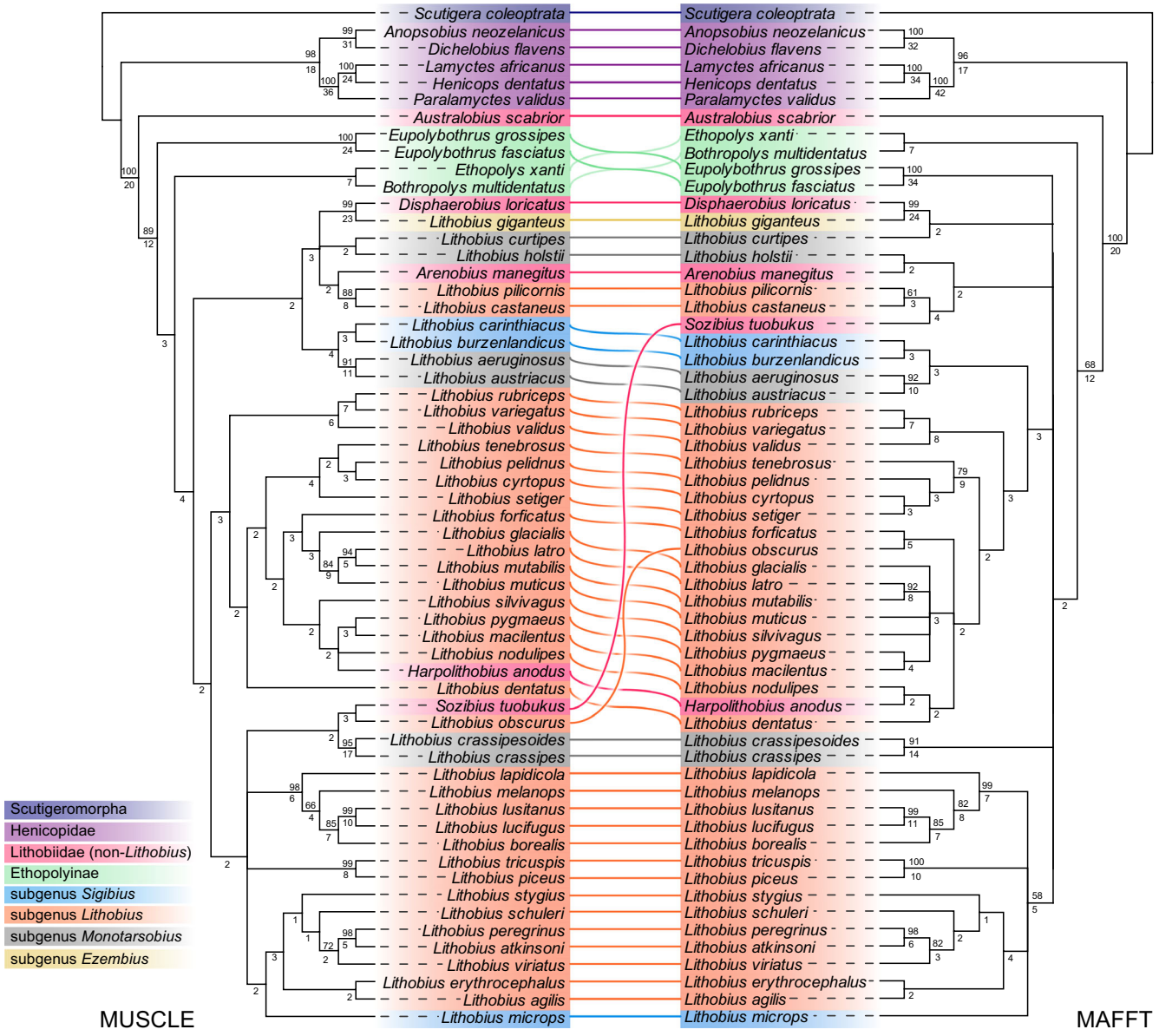

Fig. 9. Strict consensus trees from the parsimony analyses based on the morphological and all molecular data (18S rRNA + 28S + COI + 16S) with a direct comparison of the two retrieved trees using the MUSCLE (left; strict consensus of two most parsimonious trees of 7530 steps) and MAFFT (right; strict consensus of six most parsimonious trees of 7688 steps) aligned datasets. Above nodes: Jackknife frequencies >50%; below nodes: Bremer support values.

the Iberian Peninsula, and based on the similarities between both taxa, they considered *rubriceps* as a subspecies of *L. variegatus*. In the same work, they noted a few morphological differences between *rubriceps* and *variegatus*, the latter being smaller, with at least traces of posterior projections on the tergites, a dentate claw on the female gonopods, and a characteristic purple colour marking (Eason and Serra, 1986). A close relationship between these two taxa finds support in our 18S rRNA + 28S rRNA, all genes and combined analyses (Figs 5, 7, 9). However, a sister-group relationship is not resolved using the 16S rRNA + COI sequences (Fig. 6) with a genetic distance of 17.4%, higher than the minimal pairwise distance (0.3%; Supplement 6). Accordingly, we propose the restitution of *rubriceps* as full species, namely *Lithobius rubriceps* Newport, 1845, **stat.n.**, separate from *Lithobius variegatus* Leach, 1814, and recommend the revision of the Iberian specimens on that basis.

Notes on Lithobius crassipesoides *and* L. crassipes. A discrepancy in the absence/presence of internal spinulation on the mandibles (char. 31) was noted

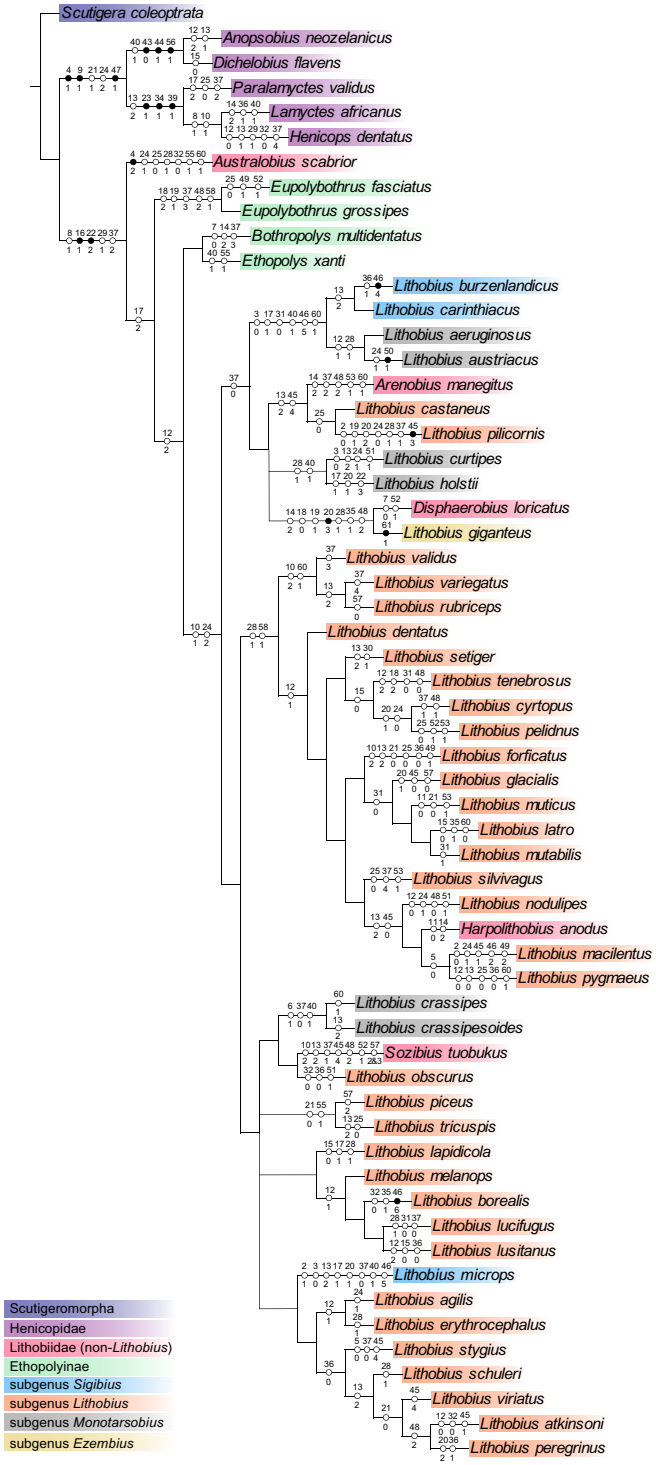

Fig. 10. One of two shortest cladograms from the parsimony analyses based on the morphological and all molecular data (18S rRNA + 28S + COI + 16S) using the MUSCLE aligned dataset under equal weights showing character optimization. Only unambiguous changes are shown, with contradicted nodes collapsed after optimizing on a fully resolved cladogram. Black circles, nonhomoplastic changes; white circles, homoplastic changes. Characters and states are numbered as in Supplement 3.

among the examined specimens of *L. crassipesoides*, for which spines were otherwise always recorded on the internal margin of the mandibles (see Fig. 4F–H). Highly doubting this character—otherwise stable in all the other lithobiid species/specimens studied with SEM—to be polymorphic, closer attention was paid to

the deviating *crassipesoides* specimen. On the one hand, in the research of Voigtländer et al. (2017), this deviating specimen clusters with the specimen (SMNG VNR17129-3) originating from the same locality as a sister group to all other sampled specimens from northern Spain (Voigtländer et al., 2017, fig. 1). On the other, the pairwise genetic distance of that specimen (SMNG VNR17129-3) to all other studied *L. crassipesoides* ranges from 12.7% to 13.3%. This value is significantly higher than the distance calculated for *L. crassipesoides*, which lies between 0.2% and 4.9% (see Supplement 10). The possibility of a cryptic speciation within *L. crassipesoides* is here hypothesized and further supported by the striking difference in the spinulation of the mandibles. However, the specimen of *L. crassipes* collected in Hungary (HNHM chilo-6186) always unites as sister taxon with *L. crassipesoides* in our phylogenetic analyses (Figs 5–7, 9). The morphological comparison of this specimen with other representatives of the species *L. crassipes* from the NHMW (see Supplement 11), specifically leg spinulation, number of coxal pores and body length, revealed important differences. In fact, the specimens used for our morphological studies perfectly fit the description of *L. crassipes* s.s. (Eason, 1964) whereas the Hungarian population (18 specimens) showed different plectrotaxies (see Supplement 11): it fits the typical leg spinulation of *L. crassipes*, especially the presence of DaP spines from leg 10 to 15 (Eason, 1964, table 13; Voigtländer et al., 2017, table 17) in two cases, but in 16 specimens some of the DaP spines are absent on legs 10–14 or even 15 in one cave specimen. Considering also the differences in the number of coxal pores and body length, we assume that these specimens may not belong to *L. crassipes* nor to *L. crassipesoides* (see Supplement 11). The pairwise distance analysis between specimens of *L. crassipes* included in our molecular analyses and other sequenced *L. crassipes* (obtained from GenBank) varies between 14.5% and 16.6% and is not resolved in a clade together with the rest of *L. crassipes* (see Supplements 10 and 12). This further supports the hypothesis of another cryptic species within the *L. crassipes-crassipesoides* species complex.

Andersson (1981) already noted the absence of DaP spines on all legs of *L. crassipes* from West Sweden even up to postlarval stadium (PL) 6–7, whereas those from South-East Sweden usually show DaP spines on legs 12 to 15, or even 5 to 15 in PL 6 to 7 (Andersson, 1981, table 4). He also observed that the younger the specimens, the higher the possibility that DaP spines are missing on the more posterior legs, even to leg 14 in PL3 (Andersson, 1981). It is questionable if the *L. crassipes* from West Sweden investigated by Andersson (1981) represent a different morph of the species or in fact another species, as already stated by himself (p. 445 therein): "However, at this stage I do not decide upon the taxonomical status of the two types (two distinct species, two subspecies or just dimorphism)."

Phylogenetic information provided by the different datasets

Information from molecular data. The 18S rRNA + 28S rRNA dataset resolves few nodes with Bootstrap support values >50% due to a rather low variation between the analyzed sequences of the genus *Lithobius* (Supplement 6). Within *Lithobius*, the taxa *L. carinthiacus* and *L. aeruginosus* are genetically distanced from their congeners based on 28S rRNA (Supplement 6) but their phylogenetic positions are neither well supported nor consistently resolved in the corresponding trees (Fig. 5). The obtained 18S rRNA data seem not to be useful for phylogenetic considerations at the genus level as there are just a few parsimony-informative sites along the ~1800 bp strand and the average pairwise distances within *Lithobius* is <1% (see Supplement 6). A low phylogenetic information value of the nuclear ribosomal genes 18S rRNA and 28S rRNA within *Lithobius* and across Lithobiidae as a whole contrasts with Henicopidae, in which these genes have long insertions that allow for the recovery of well-supported clades (Fig. 5).

In contrast to the nuclear ribosomal genes, the mitochondrial sequences used in this study—especially the 16S rRNA sequences—show more variable positions and proved to be useful for phylogenetic analyses within Lithobiidae. The ML analyses based on the 16S rRNA + COI in combination provide better resolved and more stable trees compared to the nuclear ribosomal analyses (Figs 5 and 6), with 34/36 of the 56 nodes supported with >50% Bootstrap values. The 16S rRNA + COI data help to resolve some shallower nodes within *Lithobius* and the trees support further nodes for lithobiids at the intergeneric level, in contrast to the nuclear ribosomal trees (compare Figs 5 and 6). However, some of the shallower nodes are neither well-supported nor stable across the different alignment procedures tested, which concerns, in particular, species belonging to the subgenus *Sigibius* and a large clade of species of *Lithobius* with *L. nodulipes* as sister taxon in the MUSCLE but not in the MAFFT tree (Fig. 6).

Employing different alignment procedures prior to conducting the phylogenetic analyses (see Material & Methods) resulted in different ML optimization log likelihoods and deviating topologies for all tested partitions (Table 3, Figs 5–7, 9; Supplements 4 and 5). However, well-supported nodes were mainly stable across all trees obtained, and only nodes that received low support values do not resemble each other in the

trees using different alignment procedures (see Figs 5–7, 9). In the case of our dataset, the MUSCLE alignment always received higher ML optimization log likelihoods and the shortest tree lengths (parsimony) in comparison to the MAFFT alignment (Table 3). For the 18S rRNA + 28S rRNA data, GBLOCKS was used because in both datasets long insertions in these genes within Henicopidae caused many gaps for the lithobiid taxa. Due to the different rates of evolution of gene regions, it is advantageous to use conserved blocks as they result in better identification of homologous positions and, therefore, obtaining a higher phylogenetic signal, as highlighted previously by Castresana (2000), Talavera and Castresana (2007) and references therein. The results of this investigation highlight the influence of different alignment algorithms prior to the actual analysis.

Information from morphological data. The morphological data show monophyly of Lithobiidae as hypothesized in previous phylogenetic studies (e.g. Koch and Edgecombe, 2008; Ganske et al., 2018a). Nevertheless, as already stated by Ganske et al. (2018a), the morphological data alone are not sufficient to resolve shallower nodes within the family Lithobiidae and the genus *Lithobius*. Very few nodes (i.e. *D. loricatus* and *L. giganteus*, and *E. grossipes* and *E. fasciatus*) have significant resampling support and the strict consensus is poorly resolved (Fig. 8). This is unquestionably a limitation of the taxon to character-ratio used in the present study, which results in trees with low support values and, in general, low resolution of nodes after the MP analysis. Many of the studied characters in *Lithobius* show intraspecific variability, if not phenotypic plasticity, and character optimization on the total evidence tree as well as fit statistics (CI and RI) highlight that the majority of character states are prone to homoplasy (Fig. 10). Nevertheless, a few states were identified as nonhomoplastic changes (Fig. 10). The character sample could potentially be bolstered studies on other character systems with microcomputed tomography (e.g. internal organs of the reproductive system) and, subsequently, to search those systems for more microstructural characters using transmission electron microscopy (e.g. sperm/spermatophore or accessory gland ultrastructure).

Information from the total evidence analyses. Analyzing a combination of the available molecular and morphological data using both parsimony and BI, the results for the well-supported nodes are congruent in most of cases (Fig. 9, Supplement 13), although the total evidence analyses generally resolve in favour of the molecular trees. In general, comparing the results of the morphological and molecular analyses is limited by the ambiguity of the morphological cladogram (compare Figs 8–9). As discussed above, *Australobius* as sister group to all other sampled Lithobiidae is not resolved by the morphological data but the conflicting nodes that place *A. scabrior* within Lithobiidae are all weakly supported (no Bremer support, low Jackknife values). Most of the well-supported species groups in the molecular tree and the combined tree are either not resolved or not well supported in the morphological tree (Figs 6–9). An obvious and important example of congruence between morphological and molecular signal, though, is the sister-group relationship between *L. giganteus* and *D. loricatus*, all data sources converging on the same placement of Pterygoterginae within or as sister group to *Ezembius*.

Conclusion

The present study is the first broadly sampled attempt to provide hypotheses on the phylogeny of the centipede family Lithobiidae with a sampling focus on the genus *Lithobius* based on molecular and morphological data separately and in combination. The analytical results support the following hypotheses: (i) the Lithobiidae is monophyletic and sister group to Henicopidae; (ii) the first molecular data for the lithobiid subfamilies Pterygoterginae and Gosibiinae show that they cluster within the Lithobiinae; (iii) the subfamily Ethopolyinae may be paraphyletic; (iv) molecular data and their combination with morphology support the genus *Australobius* as the sister taxon to all other sampled Lithobiidae; (v) the genus *Lithobius* is nonmonophyletic, having representatives of other lithobiid genera and subfamilies clustering within it; (vi) the subgenera *Lithobius*, *Sigibius* and *Monotarsobius* are likewise nonmonophyletic, their respective taxonomic status cannot be justified on a phylogenetic basis, and their putatively diagnostic characters are prone to homoplasy; and (vii) certain inter-relationships of species of *Lithobius* are resolved using molecular data.

This research poses many questions regarding cryptic speciation and confirms other questions already posed on the taxonomy of the family Lithobiidae, its subfamilies included in this study and the genus *Lithobius*, which need further clarification. We are aware that there could be more cryptic taxa and lineages that cannot be distinguished based on external morphological features, a known issue for different centipede taxa (Edgecombe and Giribet, 2019 and references therein). Notwithstanding these limitations, our phylogenetic results explicitly expose the artificial nature of traditional classification of lithobiids at the generic, subgeneric and in cases subfamilial levels. Transcriptomic and genomic studies at the population and species

levels are an obvious way forward for clarifying some of the problematic species-groupings and recovering better supported clades that can underpin a more phylogenetically informed classification.

Acknowledgements

This project received funding from the European Union's Horizon 2020 research and innovation programme under the Marie Sklodowska-Curie grant agreement No 642241 as part of the BIG4 project: "Biosystematics, informatics and genomics of the big 4 insect groups: training tomorrow's researchers and entrepreneurs" and a grant from NOBIS Austria (Network of Biological Systematics Austria). The authors are grateful to all colleagues who contributed collecting and/or providing valuable material for the study, particularly Anthony Barber (Ivybridge, UK), Peter Decker (Senckenberg, Görlitz, Germany), Joseph W. DeSisto (USA), Gyulli Farzalieva (Perm State University, Russia), Jürgen Gruber (NHM-Wien, Austria), Paul Marek (Virginia Polytechnic Institute and State University, USA), Prashant Sharma (University of Wisconsin-Madison, USA), Alexey Solodovnikov (Natural History Museum Denmark) and Karin Voigtländer (Senckenberg, Görlitz, Germany). Many thanks to Dan Topa (Natural History Museum Vienna, Austria) for support with the SEM and the sputter coater, to Andreas Wanninger for the access to laboratory facilities and to Christian Baranyi for support in the laboratory (both University of Vienna, Austria). The authors thank two anonymous reviewers and the associate editor Torsten Dikow for their comments, which helped to improve an earlier version of the manuscript. Thanks to the Willi Hennig Society for the free availability of their edition of TNT. Thanks to the developers for providing the following open source software: SequenceMatrix, PhyDE, MEGA, Mesquite, RAxML, MrBayes, FigTree, Dendroscope and Homebrew. This work used the Extreme Science and Engineering Discovery Environment (XSEDE), which is supported by National Science Foundation grant number ACI-1548562.

Conflict of interest

The authors have no conflicts of interest to disclose.

Appendix

The morphological character matrix of Ganske et al. (2018a) had character 46 erroneously coded for *Lithobius lapidicola*. We amended the character state from (6) to (2). Only *Lithobius borealis* expresses state (6) for this character, as clarified by Eason (1974).

References

Andersson, G., 1981. Post-embryonic development and geographical variation in Sweden of *Lithobius crassipes* L. Koch (Chilopoda: Lithobiidae). Entomol. Scand. 12, 437–445.

Bonato, L., Edgecombe, G.D., Lewis, J.G.E., Minelli, A., Pereira, L., Shelley, R.M. and Zapparoli, M., 2010. A common terminology for the external anatomy of centipedes (Chilopoda). ZooKeys, 69, 17–51.

Bonato, L., Chagas Junior, A., Edgecombe, G.D., Lewis, J.G.E., Minelli, A., Pereira, L.A., Shelley, R.M., Stoev, P. and Zapparoli, M., 2016. ChiloBase 2.0 – A world catalogue of centipedes (Chilopoda). Retrieved from http://chilobase.biologia.unipd.it.

Carpenter, J.M. and Wheeler, W.C., 1999. Towards simultaneous analysis of morphological and molecular data in Hymenoptera. Zool. Scr. 28, 251–260.

Castresana, J., 2000. Selection of conserved blocks from multiple alignments for their use in phylogenetic analysis. Mol. Biol. Evol. 17, 540–552.

Chamberlin, R.V., 1911. The Lithobiomorpha of the Southeastern states. Ann. Entomol. Soc. Am. 4, 32–48.

Chamberlin, R.V., 1917. The Gosibiidae of America North of Mexico. Bull. Mus. Comp. Zool. 57, 203–255.

Chamberlin, R.V., 1922. Further studies on North American Lithobiidae. Bull. Mus. Comp. Zool. 57, 259–382.

Eason, E.H., 1964. Centipedes of the British Isles. London, UK: Frederick Warne & Co.

Eason, E.H., 1974. The type species and identity of the species described in the genus *Lithobius* by F. Meinert, and now preserved in the Zoological Museum, Copenhagen University (Chilopoda: Lithobiomorpha). Zool. J. Linn. Soc. Lond. 55, 1–52.

Eason, E.H., 1978. On Lithobiidae from the Seychelles with descriptions of two new species of the subgenus *Australobius*, genus *Lithobius* (Chilopoda: Lithobiomorpha). J. Zool. 184, 21–34.

Eason, E.H., 1992. On the taxonomy and geographical distribution of the Lithobiomorpha. Ber. Naturwiss. Med. Ver. Innsb. Supplement 10, 1–9.

Eason, E.H., 1996. The rediscovery of *Australobius scabrior* Chamberlin (Chilopoda: Lithobiidae). Aust. Entomol. 23, 91–92.

Eason, E.H. and Serra, A., 1986. On the geographical distribution of *Lithobius variegatus* Leach, 1814 and the identity of *Lithobius rubriceps* Newport, 1845 (Chilopoda: Lithobiomorpha). J. Nat. Hist. 20, 23–29.

Edgar, R.C., 2004. MUSCLE: multiple sequence alignment with high accuracy and high throughput. Nucleic Acids Res. 32, 1792–1797.

Edgecombe, G.D., 2007. Centipede systematics: progress and problems. Zootaxa, 1668, 327–341.

Edgecombe, G.D. and Giribet, G., 2002. Myriapod phylogeny and the relationships of Chilopoda. In: Llorente Bousquets, J.E. and Morrone, J.J. (Eds.) Biodiversidad, taxonomía y biogeografía de artrópodos de México: Hacia una síntesis de su conocimiento. Prensas die Ciencias, Universidad Nacional Autónoma de México, Mexico D.F., pp. 143–168.

Edgecombe, G.D. and Giribet, G., 2003. Relationships of Henicopidae (Chilopoda: Lithobiomorpha): New molecular data, classification and biogeography. Afr. Invertebr. 44, 13–38.

Edgecombe, G.D. and Giribet, G., 2004. Adding mitochondrial sequence data (16S rRNA and cytochrome *c* oxidase subunit I) to the phylogeny of centipedes (Myriapoda: Chilopoda): an analysis of morphology and four molecular loci. J. Zool. Syst. Evol. Res. 42, 89–134.

Edgecombe, G.D. and Giribet, G., 2019. The molecularization of centipede systematics. In: Fusco, G. (Ed.) Perspectives on Evolutionary and Developmental Biology. Padova University Press, Padova, pp. 153–165.

Edgecombe, G.D. and Hollington, L.M., 2002. Morphology and distribution of *Australobius scabrior* (Chilopoda: Lithobiomorpha: Lithobiidae). Mem. Queensl. Mus. 48, 103–118.

Edgecombe, G.D., Giribet, G. and Wheeler, W.C., 2002, Phylogeny of Henicopidae (Chilopoda, Lithobiomorpha): a combined analysis of morphology and five molecular loci. Syst. Entomol. 27, 31–64.

Folmer, O., Black, M., Hoeh, W., Lutz, R. and Vrijenhoek, R., 1994. DNA primers for amplification of mitochondrial cytochrome c oxidase subunit I from diverse metazoan invertebrates. Mol. Mar. Biol. Biotech. 3, 294–299.

Ganske, A.-S., Edgecombe, G.D. and Akkari, N., 2018a. Morphology of the mandibles and the first maxillae in the family Lithobiidae (Myriapoda, Chilopoda), with remarks on their phylogenetic significance. J. Morphol. 279, 1798–1826. https://doi.org/10.1002/jmor.20902.

Ganske, A.-S., Edgecombe, G.D. and Akkari, N., 2018b. The peristomatic structures as a source of systematic characters in the genus *Lithobius* Leach, 1814 (Myriapoda, Chilopoda). In: Stoev, P. and Edgecombe, G.D. (Eds), Proceedings of the 17th International Congress of Myriapodology, Krabi, Thailand. ZooKeys. 741, 49–75.

Giribet, G., Carranza, S., Baguña, J., Riutort, M. and Ribera, C., 1996. First molecular evidence for the existence of a Tardigrada + Arthropoda clade. Mol. Biol. Evol. 13, 76–84.

Goloboff, P. and Catalano, S., 2016. TNT, version 1.5, with a full implementation of phylogenetic morphometrics. Cladistics, 32, 221–238. https://doi.org/10.1111/cla.12160, (www.lillo.org.ar/phylogeny/tnt/).

Hollington, L.M. and Edgecombe, G.D., 2004. Two new species of the henicopid centipede *Henicops* (Chilopoda: Lithobiomorpha) from Queensland and Victoria, with revision of species from Western Australia and a synoptic classification of Henicopidae. Rec. Aust. Mus. 56, 1–28.

Huelsenbeck, J.P. and Ronquist, F., 2001. MRBAYES: Bayesian inference of phylogeny. Bioinformatics, 17, 754–755.

Huson, D.H. and Scornavacca, C., 2012. Dendroscope 3 – An interactive viewer for rooted phylogenetic trees and networks. Syst. Biol. 61, 1061–1067.

Iorio, É. and Voigtländer, K., 2019. The Lithobiomorpha of the continental Iberian Peninsula (Chilopoda): new data, description of a new species of the genus *Lithobius* (s. str.), checklist and identification key. Mémoires de la Société Linnéenne de Bordeaux, Tome 18, Bordeaux.

Kaczmarek, J., 1977. *Lithobius* (*Lithobius*) *tenebrosus setiger* n. ssp. aus den polnischen Karpaten nebst Bemerkungen über die in Polen festgestellten *Lithobius* (*L.*) *tenebrosus*-Unterarten. Bull. Soc. Amis Sci. Lett. Poznan. Sér. D, 17, 221–226.

Katoh, K., Rozewicki, J. and Yamada, K.D., 2017. MAFFT online service: multiple sequence alignment, interactive sequence choice and visualization. Brief. Bioinform., 20, 1160–1166.

Koch, M. and Edgecombe, G.D., 2008. The peristomatic structures of Lithobiomorpha (Myriapoda, Chilopoda): comparative morphology and phylogenetic significance. J. Morphol. 269, 153–174.

Koren, A., 1992. Die Chilopoden-Fauna von Kärnten und Osttirol - Teil 2 Lithobiomorpha. Naturwissenschaftliche Beiträge zur Heimatkunde Kärntens, Mitteilungen des Naturwissenschaftlichen Vereins Kärntens, Sonderheft, Verlag des Naturwissenschaftlichen Vereins Kärnten, Klagenfurt, Vol. 51.

Kumar, S., Stecher, G. and Tamura, K., 2016. MEGA7: molecular evolutionary genetics analysis version 7.0. Mol. Biol. Evol. 33, 1870–1874.

Maddison, W.P. and Maddison, D.R., 2018. Mesquite: a modular system for evolutionary analysis. Version 3.40, Retrieved from http://www.mesquiteproject.org.

Matic, Z. (1966) Fauna Republicii Socialiste Romania. Clasa Chilopoda - Subclasa Anamorpha. Acad. Repub. Social. Rom., 6, 1–266.

Miller, M.A., Pfeiffer, W. and Schwartz, T. (2010) Creating the CIPRES Science Gateway for inference of large phylogenetic trees. Proceedings of the Gateway Computing Environments Workshop (GCE), New Orleans, LA, pp. 1-8.

Murienne, J., Edgecombe, G.D. and Giribet, G., 2010. Including secondary structure, fossils and molecular dating in the centipede tree of life. Mol. Phylogenet. Evol. 57, 301–313.

Newport, G., 1845. Monograph of the Class Myriapoda, order Chilopoda. Trans. Linn. Soc. Lond. 19, 349–439.

Nixon, K.C. (2004) ASADO version 1.61. Program and documentation distributed by the author. Ithaca, New York, USA.

Pilz, C., Melzer, R.R. and Spelda, J., 2008. Morphometrics and SEM analysis of the species pairs *Lithobius mutabilis* L. Koch, 1862 and *L. glacialis* Verhoeff, 1937 (Chilopoda, Lithobiomorpha). Org. Divers. Evol. 7, 270–289.

Qiao, P., Qin, W., Ma, H., Zhang, T., Su, J. and Lin, G., 2018. Two new species of *Lithobius* on Qinghai-Tibetan plateau identified from morphology and COI sequences (Lithobiomorpha: Lithobiidae). ZooKeys, 785, 11–28.

Ronquist, F. and Huelsenbeck, J.P., 2003. MRBAYES 3: Bayesian phylogenetic inference under mixed models. Bioinformatics, 19, 1572–1574.

Stamatakis, A., 2014. RAxML Version 8: A tool for Phylogenetic Analysis and Post-Analysis of Large Phylogenies. Bioinformatics, 30, 1312–1313.

Talavera, G. and Castresana, J., 2007. Improvement of phylogenies after removing divergent and ambiguously aligned blocks from protein sequence alignments. Syst. Biol. 56, 56–577.

Towns, J., Cockerill, T., Dahan, M., Foster, I., Gaither, K., Grimshaw, A., Hazlewood, V., Lathrop, S., Lifka, D., Peterson, G.D. *et al*., 2014. XSEDE: accelerating scientific discovery. Comput. Sci. Eng. 16, 62–74.

Vaidya, G., Lohman, D.J. and Meier, R., 2011. SequenceMatrix: concatenation software for the fast assembly of multi-gene datasets with character set and codon information. Cladistics, 27, 171–180.

Verhoeff, K.W., 1925. Beiträge zur Kenntnis der Steinläufer, Lithobiiden. In: Strand, E. (Ed.), Archiv für Naturgeschichte, Abteilung A, Heft 9. Nicolaische Verlags-Buchhandlung R. Stricker, Berlin.124–158.

Voigtländer, K., Iorio, E., Decker, P. and Spelda, J., 2017. The subgenus *Monotarsobius* in the Iberian Peninsula with a description of a new-pseudo-cryptic species from Northern Spain revealed by an integrative revision of *Lithobius crassipes* L. Koch, 1862 (Chilopoda, Lithobiomorpha, Lithobiidae). ZooKeys, 681, 1–38.

Whiting, M.F., Carpenter, J.C., Wheeler, Q.D. and Wheeler, W.C., 1997. The Strepsiptera problem: phylogeny of the holometabolous insect orders inferred from 18S and 28S ribosomal DNA sequences and morphology. Syst. Biol. 46, 1–68.

Xiong, B. and Kocher, T.D., 1991. Comparison of mitochondrial DNA sequences of seven morphospecies of black flies (Diptera: Simuliidae). Genome, 34, 306–311.

Zapparoli, M., 2003. The present knowledge on the European fauna of Lithobiomorpha. Bull. Br. Myriapod Isopod Group, 19, 20–41.

Zapparoli, M. and Edgecombe, G.D., 2011. Chilopoda – taxonomic overview: Order Lithobiomorpha. In: Minelli, A. (Ed.), Treatise on Zoology – Anatomy, Taxonomy, Biology. The Myriapoda, Volume I. Brill, Leiden, pp. 371–389.